NOVA SCHOOL OF SCIENCE & TECHNOLOGY

DEPARTMENT OF PHYSICS

AFONSO MANUEL CAETANO JÚLIO

Bachelor of Science in Biomedical Engineering

LINEAR AND NONLINEAR ANALYSIS OF TRUNK SWAY TIME SERIES IN OFFICE WORKERS WITH AND WITHOUT CHRONIC SPINAL PAIN

MASTER IN BIOMEDICAL ENGINEERING

NOVA University Lisbon
October, 2023

NOVA SCHOOL OF SCIENCE & TECHNOLOGY

DEPARTMENT OF PHYSICS

LINEAR AND NONLINEAR ANALYSIS OF TRUNK SWAY TIME SERIES IN OFFICE WORKERS WITH AND WITHOUT CHRONIC SPINAL PAIN

AFONSO MANUEL CAETANO JÚLIO

Bachelor of Science in Biomedical Engineering

Adviser: Hugo Filipe Silveira Gamboa

Associate Professor with Aggregation, NOVA University Lisbon

MASTER IN BIOMEDICAL ENGINEERING

NOVA University Lisbon
October, 2023

Linear and nonlinear analysis of trunk sway time series in office workers with and without chronic spinal pain

This document was created with the (pdf/Xe/Lua)LaTeX processor and the NOVAthesis template (v6.10.18) [1].

Acknowledgements

After 5 years of studying to become a Biomedical Engineer, the feeling of achievement and pride in what I accomplished is overwhelming. And for that, I would like to thank all those who helped me finish this cycle.

To my adviser, Professor Hugo Gamboa, I would like to express my gratitude, not only for the opportunity to improve my research skills and to grow as a person and a student but for all the advice and guidance given when I was feeling lost throughout the course of this work.

To Eduarda Oliosi, I thank you for never leaving a question unanswered, for all your patience, advice, support, and motivation, without which this work would not have been possible.

I extend my gratitude to the entire LIBPhys team, especially to Luís Silva and Phillip Probst. Thank you Luís, for all your patience in discussing new ideas and methods necessary for this work, for all the teachings that have allowed me to grow in scientific knowledge, and for challenging me to do more. Thank you Phillip, for all your help and for asking the right questions that I thought I had the answer to, allowing me to improve this work.

To my friends, whose unconditional support in both good and bad times has allowed me to always believe in myself and challenge myself to do and be more. Thank you.

Last but not least, my biggest thanks go to my family, to whom I dedicate this work. To my parents, for always believing in me and pushing me to be better, for giving me this opportunity, for all the support when things didn't go so well, and for the education they gave me that made me who I am today. To my sister, for the example you always were, making me want to be more like you.

Abstract

Office workers are likely to spend increasingly more time seated in their daily work but also throughout their personal lives. Public administration workers, particularly those working for tax authorities, are vulnerable to developing chronic spinal pain as a result of prolonged sitting (that affects their trunk variability).

This study presents an analysis of trunk sway time series in office workers (Tax Authority), with or without chronic spinal pain, to characterize and verify potential kinematic differences between these groups and the impact of prolonged sitting periods in the postural sway of these subjects. This analysis includes measures of variability and is carried out by applying two methods: linear (amount of variability) and nonlinear (complexity of variability). Using a smartphone, the acceleration and rotation vector time series were recorded from 16 workers.

A dashboard was created to visualize subjects' pain reports. An algorithm was developed to remove non-seated subjects' periods. Another algorithm was developed to convert the rotation vector into center of pressure displacement time series from which the time series of postural sway is extracted, based on the limits defined in the literature for the range of postural sway. Linear and nonlinear analysis is applied to these series, calculating various metrics to characterize the differences between chronic spinal pain and healthy subjects.

Results showed few statistically significant differences within and between groups. Higher values of variability for chronic spinal pain subjects were observed. Linear metrics suggested that chronic spinal pain and healthy subjects increased the trunk's variability as the day progressed, and decreased trunk's variability over the week. Results for Nonlinear metrics were inconclusive.

Keywords: Chronic Spinal Pain, Office work, Prolonged sitting, Linear metrics, Nonlinear metrics, Postural sway, Variability, Rotation vector

Resumo

Trabalhadores de escritório tendem a passar cada vez mais tempo sentados no seu trabalho, mas também ao longo das suas vidas pessoais. Os funcionários da administração pública, em particular aqueles que trabalham para autoridades fiscais, são vulneráveis ao desenvolvimento de raquialgia crónica como resultado de estar sentado durante muito tempo (que afeta a sua variabilidade do tronco).

Este estudo apresenta uma análise das séries temporais de oscilação do tronco em trabalhadores de escritório (Autoridade Tributária), com ou sem raquialgia crónica, para caracterizar e verificar potenciais diferenças cinemáticas entre estes grupos e o impacto de estar muito tempo sentado na oscilação postural destes sujeitos. Esta análise inclui medidas de variabilidade e é realizada aplicando dois métodos: linear (quantidade de variabilidade) e não linear (complexidade da variabilidade). Utilizando um smartphone, as séries temporais de aceleração e vetor de rotação foram registadas em 16 trabalhadores.

Foi criado um Dashboard para visualizar os relatórios de dor dos sujeitos. Foi desenvolvido um algoritmo para remover os períodos onde os sujeitos não se encontrava, sentados. Outro algoritmo foi desenvolvido para converter o vetor de rotação numa série temporal de deslocamento do centro de pressão, a partir da qual a série temporal de oscilação postural é extraída, com base nos limites definidos na literatura para o intervalo de oscilação postural. A análise linear e não linear é aplicada a estas séries, calculando várias métricas para caracterizar as diferenças entre os sujeitos com e sem raquialgia crónica.

Os resultados mostraram poucas diferenças estatisticamente significativas intra e inter grupos. Foram observados valores mais elevados de variabilidade para os sujeitos com raquialgia crónica. As métricas lineares sugerem que os sujeitos com e sem raquialgia crónica aumentaram a variabilidade do tronco à medida que o dia avançava e diminuíram a variabilidade do tronco ao longo da semana. Os resultados para as métricas não lineares foram inconclusivos.

Palavras-chave: Raquialgia Crónica, Trabalho de Escritório, Intervalo Sentado Prolongado, Métricas Lineares, Métricas Não Lineares, Oscilação Postural, Variabilidade, Vetor de Rotação

Contents

List of Figures

List of Tables

Acronyms

3D	Three-dimensional *(p. 8)*
4D	Four-dimensional *(p. 8)*
AM	Morning *(p. 18)*
AP	Anteroposterior *(pp. 13, 25, 28)*
CG	Control group *(pp. 19, 20, 30, 31, 33, 36)*
CLBP	chronic Low Back Pain *(p. 15)*
COP	Center of Pressure *(pp. viii, 3, 12–14, 17, 24, 25, 27, 28, 30, 33)*
CSP	Chronic Spinal Pain *(pp. 1–3, 10, 15, 16, 19, 21, 36)*
CSV	Comma Separated Values *(p. 19)*
DFA	Detrended Fluctuation Analysis *(pp. 11, 17)*
EG	Experimental group *(pp. 19, 20, 30, 31, 33, 36)*
H	Hurst Exponent *(pp. viii, 27–29, 33, 38, 39)*
IAAFT	Iterated Amplitude Adjusted Fourier Time-series Surrogates *(p. 27)*
IMUs	Inertial Measurement Units *(p. 15)*
IQR	Interquartile range *(pp. 10, 26, 30, 31, 36)*
LBP	Low Back Pain *(pp. 12, 16, 39, 40)*
MFDFA	Multifractal Detrended Fluctuation Analysis *(pp. viii, 11, 17, 26, 28)*
ML	Mediolateral *(pp. 13, 25, 28)*
PM	Afternoon *(p. 18)*
PrevOccupAI	Prevention of Occupational Disorders in Public Administration based on the Artificial Intelligence *(pp. 2, 18, 37)*
RMS	Root mean square *(pp. 10, 14, 26, 30, 31, 35, 36)*

SampEn Sample Entropy *(pp. 10, 13–15, 26, 29, 33)*

SD Standard deviation *(pp. x, 10, 13, 14, 16, 17, 26, 28–31, 36, 52, 55, 58, 61)*

TSFEL Time Series Feature Extraction Library *(p. 18)*

Chapter 1

Introduction

1.1 Context and Motivation

The work environment is the place where people spend, not only most part of their daytime but also their life. Office workers, for example, are subjected to long periods of sitting, and if the working environment does not present good conditions, this can lead to muscle stiffness and fatigue. Constant exposure to these factors might lead to the development of pathologies [2]. The overall tendency of prolonged sitting periods is increasing as people spend more time at work so, it is mandatory the existence of safe and comfortable working conditions [3]. An EU-wide Survey on New Emerging Risks in Enterprises identified prolonged sitting as the second most frequent risk factor, being estimated that 39% of workers complete their tasks while seated [4].

Office workers, like the ones from tax authorities for example, have increased vulnerability to develop Chronic Spinal Pain (CSP) resulting from prolonged sitting [3]. These workers have to execute a wide range of operational tasks (tax collection, detection of tax avoidance, and fraud), leading to an accumulation of time seated. These factors lead to workers being exposed to higher levels of stress resulting from these tasks, affecting work performance in several ways: job satisfaction might decrease; a loss in productivity can arise due to health issues and work attendance might decrease [5]. Prolonged sitting periods lead to an increase in discomfort [3, 6, 7] and affect the movement variability [7–10].

CSP is a pathology affecting the world population and is known to be responsible for causing disability, having a major impact on individuals' well-being and daily lives. According to the International Association for the Study of Pain (IASP) and the International Classification of Diseases (ICD-11) in 2019, a disease is considered chronic if the pain persists or recurs for at least three months [9, 11–14]. Up to 85% of people affected

by CSP suffer with ongoing pain for several years following their first recorded episode [12], presenting this condition a higher probability of persistence and recurrence. The majority of patients diagnosed with CSP present nonspecific symptoms with no obvious pathological changes [15]. This shows that CSP is a complex pathology with significant inter-subject differences. The individual pain experience is inherently multifactorial, meaning that biological, physiological, and psychosocial factors can contribute to it in varying degrees. Therefore, when assessing and managing CSP and other pain-related chronic diseases, a holistic view, that acknowledges the condition as a biopsychosocial phenomenon, has to be applied [12, 16]. Furthermore, this chronic pathology is responsible for large socioeconomic costs, not only from medical treatment expenses but also from work absenteeism, having long-term consequences that negatively impact the ability to perform daily activities [9, 12, 14, 17–21]. The growth in the prevalence of CSP in the future is expected to rise since the workforce is aging, the retirement age is increasing, and more sedentary work is the ongoing trend [4, 14].

Therefore, it is essential to develop tools that can facilitate a better understanding of the clinical course and complexities of this condition and create affordable and user-friendly technologies that allow the identification of individuals suffering from this pathology. This would enable health professionals to achieve a faster diagnosis without increased expenses, a faster start for treatment, and better adjustment to the pathology [21].

The present thesis is part of the Prevention of Occupational Disorders in Public Administration based on the Artificial Intelligence (PrevOccupAI) project [22], which has the support of the Portuguese Autoridade Tributária e Aduaneira (AT) and Direção-Geral da Saúde (DGS). This project aims to prevent occupational diseases in the office context, through the identification of risk factors, in order to promote occupational health.

The research work described in this dissertation was carried out in accordance with the norms established in the ethics code of Universidade Nova de Lisboa. The work described and the material presented in this dissertation, with the exceptions clearly indicated, constitute original work carried out by the author.

1.2 Objectives

CSP has a high prevalence in office workers, presenting changes in posture [4, 14]. However, there is no information on how postural variability changes during a working week in individuals who suffer from CSP compared to healthy ones. Therefore, the main objective of this thesis is to analyze the real-time trunk dynamics (postural sway) of individuals with pathology (i.e., CSP) and compare it to healthy individuals during computer work tasks. To test the hypothesis that workers with CSP will exhibit decreased trunk variability during real-time computer work, time series data, including acceleration and rotation vectors, collected during the PrevOccupAI project were analyzed. To achieve the final goal, both linear analysis (commonly used for studying postural sway in individuals

with pathology [7, 23–25]) and nonlinear analysis of the COP time series were performed. Furthermore, specific objectives are also to be tested:

1. Explore the impact of prolonged sitting during work in office workers with and without CSP;
2. Compare the amount of trunk's movement variability between CSP and no CSP office workers;
3. Compare the complexity of the trunk's movement variability between CSP and no CSP office workers;
4. Verify if there are changes in the postural sway of both healthy and CSP subjects during the working day/week.

Signal pre-processing and cross-validation were also performed to meet the aforementioned objectives. This thesis will help better understand CSP motor patterns by contributing with computational tools to analyze new potential indicators and measures.

1.3 Structure

This thesis consists of six chapters, each divided into multiple subsections. Chapter One outlines the context and motivation for this study, as well as its primary objectives. Chapter Two describes the essential theoretical concepts necessary for understanding this thesis. Chapter Three presents a literature review on the topic. Chapter Four introduces and describes the methodology used to achieve the objectives. Chapter Five presents the results obtained. Chapter Six discusses the results and highlights the main conclusions.

Chapter 2

Theoretical Concepts

2.1 Chronic Spinal Pain

Spinal pain is a common health condition that can be caused by various factors, such as inflammation, structural changes, biomechanical consequences, diseases of the nervous system, injury, herniated discs, arthritis, and other medical conditions [27]. Nevertheless, most people affected by spinal pain exhibit nonspecific symptoms that lack any distinct pathological alterations [26]. If the spinal pain lasts or recurs for a minimum of three months, even with appropriate treatment and management, is considered a chronic disease. In such cases, the condition may require more specialized and long-term management strategies. Seeking medical attention and following a comprehensive treatment plan that combines various therapies, such as medication, physical therapy, exercise, and other interventions, is crucial for managing CSP effectively [28].

2.2 Movement Variability and Postural Sway

Human movement variability is described as the normal variation that occurs in motor performance over consecutive repetitions of tasks [29]. When performing the same task multiple times, variations in kinematic, kinetic, and muscular activation patterns are observed [30]. This variability is inherent in all biological systems and can be easily observed. When a person reproduces the same movement multiple times, the two actions are never identical or independent [31]. Therefore, human movement is a complex behavior influenced by interactions among physiological systems. These interactions are crucial for maximizing an individual's functional capacity and performance, which enable them to engage with and respond to their environment effectively[31–33].

The variability in the human movement system's output provides essential information

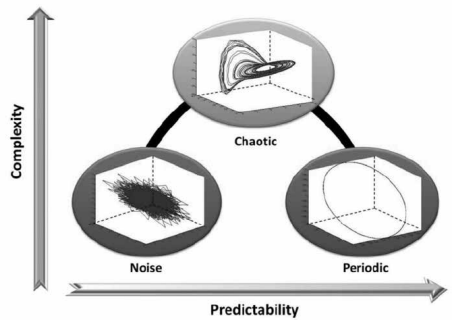

Figure 2.1: U-shaped correlation between chaotic temporal fluctuations and predictability [35].

about the overall health of underlying physiological systems, as seen through various physiological and performance measures such as heart rate, respiratory rate, postural sway, and gait strides [33]. For instance, during quiet standing, the body naturally sways around a central equilibrium point to maintain balance and spatial orientation. This means that even when we try to stand still, there will be small variations in our body position as we continuously adjust to maintain balance. These variations are a normal and essential part of the human movement system [32].

Biological systems that become rigid and unchangeable typically experience a decrease in variability, while a significant increase in variability can lead to randomness and instability. Both rigidity and instability can reduce the adaptability of the system to perturbations or changes in the environment. This means that the system becomes less flexible and less able to respond effectively to new demands. It is essential to maintain an appropriate level of variability to ensure the adaptability and resilience of the biological system to different stimuli [34].

2.3 Sensors

2.3.1 Inertial Sensors

The optimum human movement displays complex, nonlinear fluctuation patterns in motor performance during multiple repetitions of a task, indicating the organism's ability to adjust to changes in environmental conditions [33]. This optimal range of movement variability exhibits an inverted U-shaped correlation between chaotic temporal fluctuations and predictability, presenting its optimal state in the middle region, represented in Figure 2.1 Within this model, the ideal state of movement's health in biological systems is characterized by chaotic temporal fluctuations in the output state that is achieved when values lie within the intermediate range, situated between excessive order (resulting in the highest predictability) and excessive disorder (leading to a lack of predictability) [31, 33]. This model is important in health studies since optimal variability is destroyed, there is a loss in complexity and it becomes more or less predictable [32].

Inertial sensors are devices that can provide linear and angular motion information along one or more axes. The most common types of inertial sensors include an accelerometer and a gyroscope [36].

A typical inertial sensor operates based on a mass-spring system, where a mass is suspended within a mechanical framework and an input force, representing the physical parameter to be measured, induces a displacement in the mass, which is then measured. Depending on the specific sensor type, various transduction methods are employed to convert a physical quantity into a force that acts upon the mass [37]. In addition, unwanted forces also act on the mass, such as those related to different types of motion and damping. A high-quality sensor should be able to reject these undesirable forces [37]. A coordinate system must be established to use body motion measurement sensors. When dealing with a coordinate system in motion, the inertial force (F) can be expressed as follows:

$$\mathrm{F} = -mA_0 + 2mu' * \omega + m\omega * (r' * \omega) + mr' * \frac{d\omega}{dt} \tag{2.1}$$

with A_0: acceleration; ω: angular velocity; r': position vector and u': velocity of a mass m. Acceleration linked to the linear inertial force, as well as apparent forces like the Coriolis and centrifugal forces are described by the right elements of the equation [38].

2.3.1.1 Accelerometer

Following Newton's second law, the relationship between the force (F) that acts on a mass (m) is given by:

$$F = ma \tag{2.2}$$

with a being the acceleration of linear motion.

An accelerometer is a type of inertial sensor that can measure linear acceleration, typically expressed in units such as g (gravitational force) or m/s^2 (meters per second squared), where 1 g is approximately equal to 9.81 m/s^2, corresponding to the Earth's gravity. Consequently, a multi-axis accelerometer can discern the orientation of gravity and the linear acceleration resulting from movement [37]. Figure 2.2a provides an illustration of a triaxial accelerometer's signal. By integrating accelerometer data over time, it becomes possible to obtain velocity and position. The reverse process, obtaining acceleration from such data, is also possible but is susceptible to significant noise [38].

The beam-type accelerometer, depicted in Figure 2.2b, is a prevalent type. It includes an elastic beam connected to a base, with a seismic mass attached at the other end. This design allows for the measurement of mass displacement caused by acceleration. Different techniques, like capacitance measurement, offer high sensitivity, making it a valuable tool in accelerometer technology [36]. Within a piezoresistive accelerometer exists a cantilever beam equipped with a piezoresistive component. As a result, the resistance varies in accordance with the bending of the beam in response to acceleration [38].

Nowadays, most accelerometers utilize Microelectromechanical Systems (MEMS) technology. For instance, smartphones often incorporate a triaxial accelerometer based on

MEMS, providing a compact and sensitive system that can determine acceleration magnitude and direction in three-dimensional space [38].

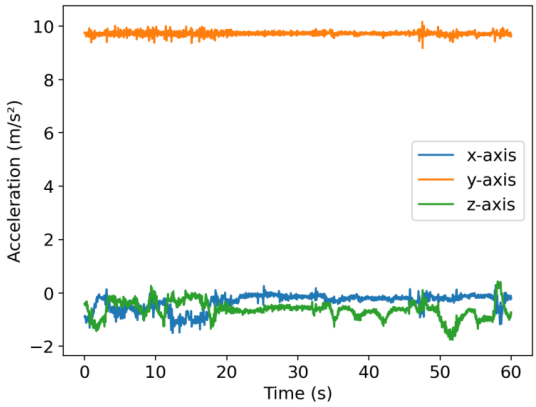

(a) Accelerometer signal of a seated person.

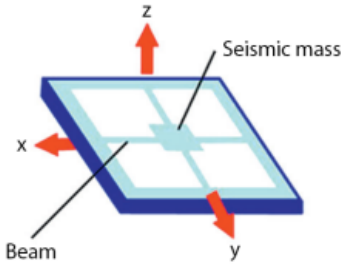

(b) Beam-type triaxial accelerometer. Adapted from [38].

Figure 2.2: Example of accelerometer signal and sensor.

2.3.1.2 Gyroscope

A gyroscope is an inertial sensor designed for measuring angular motion, typically expressed in units such as degrees per second (deg/s) or radians per second (rad/s), as shown in Figure 2.3a. When the data from the gyroscope is integrated, it allows for the calculation of angle measurements. A common gyroscope comprises a spinning wheel attached to a mobile frame. When the direction of the axis is altered, a torque is generated that is directly proportional to the rate of rotation of the axis. This fundamental principle can be applied to gauge angular velocity [38].

However, most smartphones incorporate a gyroscope that operates on a vibratory principle, utilizing MEMS technology. In this type of gyroscope exists a vibrating proof mass. When a rotation occurs along an axis perpendicular to the vibratory axis, it induces a Coriolis acceleration in proportion to the rotation, which is then detected and measured [38]. This Coriolis acceleration (a_{cor}) is given by:

$$a_{cor} = 2v_{pm} * \Omega \tag{2.3}$$

with v_{pm} being the velocity of the proof mass and Ω the rate of rotation [38]. In order to accurately determine the rate of rotation, it is essential to have precise knowledge of the velocity of the proof mass. Therefore, a vibratory rate gyroscope employs electronic means to induce controlled oscillations of the proof mass along a direction parallel to the surface of the chip, ensuring a consistent and well-known velocity. When rotation occurs in the perpendicular direction, the Coriolis force leads to the displacement of the mass in that particular direction. This displacement generates a measurable voltage, allowing for the determination of angular velocity [37, 38].

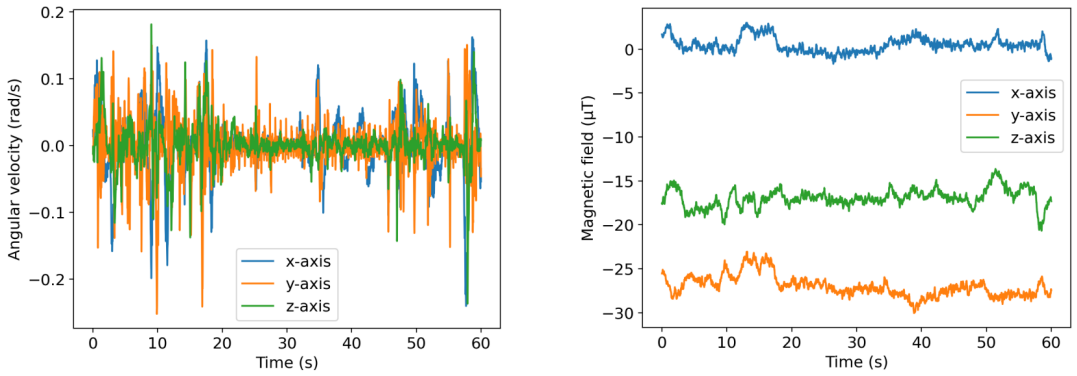

(a) Gyroscope signal of a seated person.

(b) Magnetometer signal of a seated person.

Figure 2.3: Example of gyroscope and magnetometer signals.

2.3.2 Magnetometer

A magnetometer is a sensor designed for the measurement of magnetic fields, including the Earth's magnetic field and magnetic fields produced by nearby magnetic materials [39]. Typically, magnetometers are used in conjunction with accelerometers and gyroscopes to track body movement and orientation, as exemplified by the smartphone's rotation vector sensor [38, 39]. Assuming that the sensor's movement is relatively limited compared to the Earth's size, we can treat the Earth's magnetic field as relatively constant. Consequently, when there are no magnetic materials in proximity to the sensor, the magnetometer can provide orientation information in conjunction with accelerometer and gyroscope data [39]. An example of a magnetometer signal is illustrated in Figure 2.3b.

Commonly used magnetometers operate on the principle of the Hall effect, which involves the interaction between mobile electrons and an external magnetic field. This interaction results in the creation of magnetic impedance and resistance. When an electron moves through a magnetic field, it experiences a force (F) defined as follows:

$$F = qvB \tag{2.4}$$

with q being the electronic charge, v the electron's speed, and B the magnetic field [38]. Similar to the inertial sensors, the magnetometers found in smartphones also utilize MEMS technology. Typically, smartphones and similar devices are equipped with three-axis magnetometers [40].

2.3.3 Rotation Vector

The rotation vector sensor merges accelerometer, gyroscope, and magnetometer data, and it is based on the mathematical concept of quaternions, which is the description of Three-dimensional (3D) orientation using a Four-dimensional (4D) complex number system [41].

A rotation vector sensor provides information about the orientation of the device relative to the East-North-Up coordinate system. The East-North-Up coordinate system is defined as a right-handed orthonormal basis where:

1. X points east and is tangent to the ground;
2. Y points north and is tangent to the ground;
3. Z points upward toward the sky and is perpendicular to the ground.

The orientation of the phone is represented by the rotation required to align the East-North coordinates with the phone's coordinates [41]. Thus, the smartphone's rotation vector returns four values that describe the phone's orientation relative to the phone's base coordinate system. An example of a rotation vector time series can be observed in Figure 2.4a and the smartphone's reference axes are illustrated in Figure 2.4b.

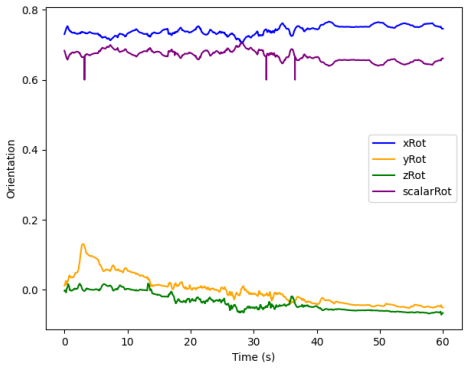

(a) Rotation vector signal of a seated person.

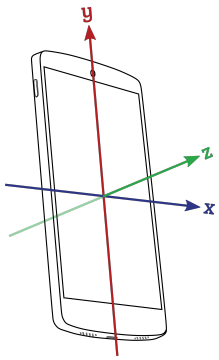

(b) Smartphone's axis [41].

Figure 2.4: Example of gyroscope and magnetometer signals.

2.4 Parameters for the Biopsychosocial Model

Chronic pain is a complex phenomenon that involves various factors, including biological, psychological, and social aspects. To better understand this phenomenon, the biopsychosocial model was introduced, which suggests that a person's health outcomes are influenced by multiple factors. This model recognizes that the interaction between biological, psychological, and social factors plays a crucial role in determining a person's overall well-being, and no single factor can solely determine a person's health status [16, 23, 42]. The biological component of the model includes factors such as genetics, physiology, and health conditions. The psychological component includes factors such as emotions, thoughts, and behaviors. The social component includes factors such as cultural beliefs, socioeconomic status, and social support networks[23, 43]. For example, a person's genetics may predispose them to certain health conditions, but their environment and social circumstances can also play a significant role in the development and management

of these conditions. Similarly, a person's psychological state can impact their physical health, and social factors can influence both psychological and physical well-being [42].

2.5 Linear Tools and Nonlinear Tools

According to Harbourne and Stergiou [32], linear measures are statistical measures that describe the average or dispersion of values within a set of numbers. These measurements are often employed in linear statistical techniques to analyze variability and quantify the extent of movement variation. In the clinical domain, linear measurements are extensively used to predict and solve arising problems. Notably, while these measurements are useful, they have limits in identifying the underlying variability structure. This constraint stems from their exclusive emphasis on one-dimensional straight-line representations [32]. Linear approaches were ineffective in dealing with the temporal structures inherent in physiological and psychological events [44]. Numerous linear metrics have been investigated by researchers to try to quantify the amount of movement variability [45], including SD, range, Root mean square (RMS), coefficient of variation, and Interquartile range (IQR).

Nonlinear measures, on the other hand, are statistical measures that quantify the relationship or dependency of numbers in a time series, describing the patterns or structure of the data rather than just the quantity. As a result, nonlinear measurements provide additional information and aid in the understanding of complexity [32]. Nonlinear statistical techniques consider additional information about a system's time-dependent structures encoded in a movement sequence. This allows for the quantification of structural variability and provides insight into a biological system's adaptability to changing environments. Nonlinear measurements are particularly relevant for measuring the functional flexibility of the trunk in the presence of CSP during cyclic movement performance [23].

2.5.1 Sample Entropy

Entropy is a nonlinear metric used to characterize information loss in a time series or signal [46]. According to Karimi et al. [47], entropy variables extracted for the time series are often used to assess the variation of series patterns with time. It is calculated as the natural logarithm of a conditional probability and can be understood as the rate of information creation, providing an estimate of the complexity of the underlying system responsible for the observed dynamics [7, 46]. Sample Entropy (SampEn) is a unitless, non-negative value that characterizes the structural irregularity or complexity of a time series and has found application in the study of kinetic or kinematic signals [48].

2.5.2 Multifractal Detrended Fluctuation Analysis

The fundamental concept underlying Fractal Analysis is the presence of self-similarity, wherein an object, when repeatedly broken down into smaller scales, exhibits consistent

similarity regardless of the scale's size. This idea also applies to time series data, where consecutive events that occur over time (e.g., ECG RR intervals or postural sway direction) can be partitioned into various window lengths, referred to as lags or scales. If the oscillations within these scales are similar, it indicates that the time series has a fractal structure [44, 49–52].

Detrended Fluctuation Analysis (DFA) can be used to evaluate the occurrence of long-range correlations in nucleotide sequences or time series [53]. The presence of long-term correlations, or memory, within a time series, implies interdependence among occurrences while retaining variability. DFA operates under the assumption of a monofractal structure, implying the existence of a single power law [50]. However, this assumption proves overly restrictive when applied to the complexities of human behavior since fractal scaling remains temporal and spatial invariant. To overcome this issue, MFDFA employs a variety of scaling orders to reveal information about both minor and large variations. A multifractal spectrum of power law exponents characterizes these geographical and temporal fluctuations [51, 52]. In addition, Surrogate analysis complements the multifractality studies. This analysis involves comparing a specific characteristic of the data with the distribution of the same characteristic computed across a series of artificially generated signals (surrogates). These surrogates are designed to mimic the original time series but lack the particular property under examination [54]. By applying the surrogate analysis to the time series, two hypotheses are to be tested:

1. Null Hypothesis (H_0): The observed fractal characteristics (or nonlinearity) in the original time series are due to linear stochastic processes that can be captured by the surrogate data. In other words, the original time series does not contain any genuine fractal characteristics (or nonlinearity) that are different from what can be observed in linearly correlated noise.

2. Alternative Hypothesis (H_1): The original time series contains genuine fractal characteristics (or nonlinearity) that are not present in the surrogate data. In other words, the fractal characteristics (or nonlinearity) in the original time series are not merely a result of linear processes but indicate the presence of genuine nonlinear dynamics or fractal structures.

Chapter 3

Literature Review

3.1 Movement Variability

Movement variability has been recognized in biomedical research as an important parameter in preventing musculoskeletal disorders [9, 55–57]. The use of variability analysis has become increasingly widespread due to its efficacy in quantifying variations in movement performance from a state of well-being to patterns of disability [31]. According to Stergiou and Decker [31], variability encompasses what can be described as the *deterministic structure*, indicating the system's capacity to adapt to environmental stimuli and stressors. Conversely, the *loss* of optimal variability results in a more predictable and rigid system, resembling robotic movement behavior [31–33, 58].

Thus, several studies dedicated their focus to finding a correlation between various markers and postural sway: Roerdink, Hlavackova, and Vuillerme [59] focused on COP regularity as a marker for attentional investment in postural control; Gizzi et al. [60] concluded that people with low back pain show reduced movement complexity during their most active daily tasks; Shahvarpour et al. [61] studied the relationship between trunk postural movement and low back pain where results suggested that only the quality (not the quantity) of movement may have relationship with pain and disability; Longo et al. [62] evaluated the differences in the movement behavior and variability between subjects with and without work-related pain finding an increase in movement variability in subjects with pain; Nishi et al. [63] found that Chronic Low Back Pain (LBP) patients exhibit changes in trunk variability and stability of gait depending on the environment, and these changes are related to pain, fear, and quality of life scores.

3.2 Analysis of Movement Variability and Postural Sway in Pathological Cases

This literature review delves into the realm of movement variability and postural sway within pathological cases of spinal pain. Chronic spinal pain is a pervasive condition known to significantly impact an individual's movement and postural stability. To shed light on this aspect, existing research is examined to understand how movement variability and postural sway in individuals with chronic spinal pain compared to healthy subjects.

Individuals with spinal pain may experience a decrease in their spinal movement control, which is characterized by natural variations in trunk movement relative to other segments, such as the pelvis [23]. To determine the habitual spinal posture of people with cervical pain, Mingels et al. [64] conducted a 30-minute standardized laptop task using 3D-Vicon motion analysis to collect data. The findings showed that individuals with cervicogenic headaches had lower average spinal movement variability across each spinal segment, compared to the control group [64]. It has been observed that there are distinct differences in the motor characteristics of different groups of individuals who suffer from spinal pain. As a case in point, it has been observed by Bontrup et al. [65] that sitting behavior is more closely related to chronic than acute low back pain. Furthermore, it has been suggested that individuals with chronic lower back pain may be more likely to engage in static sitting behavior than those without pain [65].

In research aimed at gaining deeper insights into the control mechanisms underpinning the assessment of postural control during seated activities, a study was conducted employing a force platform. This study involved the periodic collection of body part discomfort ratings at 5-minute intervals, utilizing a 6-level scale ranging from 0 to 5. To comprehensively evaluate the postural control dynamics, the displacement of the COP in both the Anteroposterior (AP) and Mediolateral (ML) directions was tracked over time. Additionally, key statistical parameters such as the mean, SD, and SampEn of COP displacement in these directions, as well as lumbar curvature, were calculated. The SD was utilized to quantify the extent of movement variability, while SampEn served as a measure of the complexity inherent in maintaining postural control during sitting. Notably, the study did not uncover any significant correlations between discomfort levels and the mean values of COP displacement or lumbar curvature. However, a positive correlation was observed between discomfort and the SDs of COP displacement in both the AP and ML directions, as well as lumbar curvature. Conversely, SampEn displayed a negative correlation with discomfort levels. Consequently, these findings suggest a discernible relationship between perceived discomfort and the increase in variability, along with a decrease in the complexity of the postural control maintained during seated activities [7].

In the study conducted by Madeleine [24], discomfort ratings, alongside kinetic and kinematics data, were recorded before and after a 96-minute working session. To measure the displacement of the COP and lumbar curvature, a plate platform and camera system

were employed. Various statistical metrics, including RMS, SD, and SampEn, were calculated from the COP and lumbar curvature signals. These metrics were used to evaluate the magnitude (RMS), degree of variability (SD), and regularity/temporal structure (SampEn) of sitting dynamics. Notably, the results of the study revealed a significant increase in discomfort in the buttocks after prolonged sitting. Furthermore, both the AP and ML displacement of the COP, as well as the SD of the lumbar curvature, exhibited an increase. Conversely, SampEn values showed a decrease. Interestingly, the RMS remained unaltered after an extended period of constrained sitting, suggesting that prolonged sitting primarily impacts the variability (SD) and regularity (SampEnn) of postural control while leaving the magnitude (RMS) unchanged [24].

A significant amount of research has been conducted to investigate the effects of prolonged seated computer work over prolonged periods, as evidenced by multiple studies [7, 24, 64, 66]. In a laboratory experiment, younger and older computer users were compared to assess the influence of age on sitting dynamics during a 40-minute computer task. To achieve this, researchers employed an instrumented office chair to capture various COP parameters, including range, velocity, area, SD, and SampEn. Results showed the older group of computer users exhibited greater COP displacement in the AP direction in terms of range, velocity, and area. In addition, both SD and SampEn values were observed to be higher and lower, respectively, for the older group in both the AP and ML directions when compared to their younger counterparts. Hence, this study suggests that prolonged computer-related sitting tasks result in increased variability and reduced complexity among older computer users [66].

Postural sway is a parameter that can be used to assess the movement's variability of sitting and standing positions. It can be quantified by tracking changes in the COP's position or the linear acceleration of body segments. Postural sway represents the integration of various sensorimotor processes, including inputs from visual, vestibular, and proprioceptive sources. In individuals experiencing neck pain, an increase in postural sway, specifically the excursion of the COP, and has been observed to be associated with higher pain intensity [67]. Additionally, increased variability in seated postural sway, as measured by the SD of the COP's location or the frequency of postural shifts, has been linked with reports of bodily discomfort among healthy subjects [7, 68].

It is essential to establish specific criteria for the analysis of quantifiable data within the movement control domain. To this end, Voss et al. [69] developed a comprehensive set of reference values by utilizing the APDM MobilityLab® inertial sensor system, specifically targeting individuals aged 5 to 30 years. Their study outcomes reveal a notable decline in all assessed sway parameters as age increases [69]. Prior investigations have delved into the influence of age, gender, and task complexity on postural sway, particularly focusing on how these variables impact the capacity of the body to maintain balance across different stance conditions. The findings suggest that postural sway patterns are relatively consistent between genders in younger participants, but among older individuals, males tend to exhibit greater sway compared to females in 10 out of 21 measured outcomes. This

observation implies that alterations in postural sway associated with the aging process are influenced by both the participant's gender and the level of task difficulty [70].

Previous studies were limited in scope and focused mainly on specific tasks performed in controlled environments. However, there is an increased need to focus on the study of movement strategies during real-time work tasks, particularly in the context of wearable sensors and information from both pain-experienced and non-pain-experienced workers.

3.3 Sensors

Recent studies have turned to more accessible biomedical instrumentation, such as Inertial Measurement Units (IMUs), as alternatives to traditional platforms and cameras. IMUs provide cost-effective solutions for investigating movement variability and postural sway.

IMUs have become a popular tool for researchers as they provide us with valuable information regarding angular rotation, which is obtained from gyroscopes that are embedded within these units. Additionally, IMUs can be utilized to calculate postural sway while performing unstable equilibrium tasks such as sitting on a wobble chair. It has been proven to be a cost-effective and valid alternative to more expensive measures of postural sway [28]. Human balance and body sway can potentially be used as a quantitative indicator of CSP's presence [19].

In addition to postural sway studies, IMUs have also been used to measure spinal movement variability by measuring trunk angle during voluntary repeated trunk movements in any plane. Other studies have used IMUs as devices for data acquisition, for example, the spinal movement variability can be studied by measuring trunk angle using these sensors during voluntary repeated trunk movements in any plane [23]. The time series data collected from different sensors can be analyzed to measure the angular velocity and acceleration of two distinct anatomical reference points. IMUs can record time series data that can be used, for example, to calculate SampEn, a nonlinear measure applicable to both healthy individuals and patients with CSP. According to a study by Thiry et al. [21], in 2022, the SampEn of patients with chronic Low Back Pain (CLBP) was reported to be lower than that of healthy subjects, indicating a loss of movement complexity due to CLBP.

Nowadays, inertial sensors are widely used for fall detection [71] as well as in recognition of human movement and activities [72, 73]. These sensors are commonly integrated into devices like smartphones and smartwatches.

3.4 Smartphone

Previous research has emphasized the usefulness of sensors that are conveniently accessible for evaluating postural control [74]. These sensors represent a valuable option, particularly for office workers, given the limited variation in biomechanical exposure

within such settings. Several investigations have demonstrated the efficacy of smartphone sensors for postural assessments, with smartphone accelerometry exhibiting comparability to the established gold standard, the force plate [75–77]. Furthermore, it has been shown to be on par with other advanced technologies employed in previous posture assessment studies [78].

3.5 Biopsychosocial Model

Movement control can be affected by various factors, including biological, psychological, and social factors (known as the biopsychosocial model). One such factor is the impact of pain and stress. A study conducted on individuals suffering from non-specific LBP found a correlation between fear of pain and variability of postural responses, which has been supported by subsequent research studies. For example, Saito et al. [23] showed that LBP patients are associated with mild-to-moderate fear of movement. Based on Hamid et al. [79], this study attends to the need to have information regarding fear of movement. CSP often results in fear of movement, which, in turn, causes patients to restrict and limit their daily activities and social interactions to avoid pain [21, 34]. To examine the ability to differentiate between chronic and No CSP subjects, it is suggested to use the biopsychosocial model as proposed by Thiry et al. [21] in studies of CSP.

To summarize, it is widely acknowledged CSP can affect a person's psychosocial well-being. Studies have shown that low pain self-efficacy, which is the belief in one's ability to manage pain, is a common factor in those with CSP [80]. Those with CSP and low pain self-efficacy are more likely to experience higher levels of pain intensity, disability, and fear avoidance beliefs [81, 82]. Therefore, assessing a person's pain self-efficacy is crucial in managing CSP.

3.6 Linear and Nonlinear Analysis

Using linear measures like SD, coefficient of variation, and coefficient of multiple correlations limits our ability to fully understand the range of variability that can give us insight into how individuals adapt to functional skills [32, 34].

Nonlinear methods can be used to characterize the structure of variability in movement behavior, which is better captured by examining the temporal organization of the distribution of relevant values. These methods measure the extent to which values appear in an ordered and predictable manner across a range of time scales and require the use of mathematical equations and software to analyze time series data [32].

Investigations into human movement mechanics traditionally employ linear mathematical approaches. While these methodologies offer valuable insights, they often fall short of capturing the intricate nonlinear characteristics inherent in human systems. Consequently, there has been a growing interest in the application of nonlinear analysis techniques within a dynamical systems framework [83].

Conventional measures of variability, such as the SD or range, are typically oriented around the mean value and its associated variability. Consequently, this approach often designates the mean as the benchmark, implying that any deviation from it is categorized as an error, as indicated by previous studies [31, 58].

In contrast, the characterization of variations within a time series in terms of their structure or organization relies on nonlinear system measures, including DFA, entropies, and the largest Lyapunov exponent, among others. Each of these metrics offers unique insights into various aspects of the temporal structural characteristics exhibited in the time series [31, 58]. However, to obtain meaningful insights into the underlying dynamics of the time series and ensure the reliability of the findings, it is imperative to consider varying minimum sample sizes for the aforementioned nonlinear measures, as suggested in the literature [32, 56].

Adding complexity to movement behavior analysis, several researchers have incorporated nonlinear parameters to assess an array of elements like discomfort [7, 24], and, within the occupational context, their interrelation with cognitive functions and the process of aging [66]. Employing optical motion capture technology, as demonstrated by Lau, Choy, and Chow [84], the performance of movements manifests multifractal attributes suggesting a correlation between multifractal behavior, indicative of diverse strategies in the control of movements and neural processes, and the assessment of the dynamic characteristics of spinal curvature during the postural oscillation, facilitated through the application of MFDFA.

In light of this, it is imperative that when evaluating time series data derived from the COP for the assessment of movement variability, comprehensive consideration of both linear and nonlinear metrics is warranted [23, 32].

Chapter 4

Methods

4.1 Computational Methods

The code needed to achieve the goals of this thesis was developed using the Python programming language through the PyCharm environment. The use of several Python libraries allowed this code development, being the most important NumPy [85], SciPy [86], pandas [87], streamlit [88], Time Series Feature Extraction Library (TSFEL) [89], fathon [90] and EntropyHub [91].

4.2 Data Acquisition

The data used in this thesis is part of the PrevOccupAI project, which used non-intrusive sensors and several questionnaires in the line of the biopsychosocial model [92], which allowed the comprehensive assessment of workers' potential occupational risks. A series of data acquisitions were carried out over five consecutive days. A detailed description of the acquisition protocol operated can be found in previously published work [22]. It is worth noting that the multimodal assessments considered the biopsychosocial model as a basis for the acquisition. However, the data lacks a ground truth to validate the observed displacement phenomenons, so some considerations were made.

4.3 Dashboard Creation for Visualization and Choosing of the Control/Experimental Group Based on Pain Reports

Over the five days of data acquisition, the subjectively experienced pain levels of each participant were recorded twice a day (Morning (AM) and Afternoon (PM)). This was done by letting participants color in a body map with different colors that corresponded

to different pain intensity levels. The coordinates and intensity of the colored parts of the image were saved into a Comma Separated Values (CSV) file. The body was divided into several regions with the attribution of coordinate intervals to these parts. Also, the hexadecimal color code was converted into numbers to establish a correlation between color and pain intensity, where the less intense color corresponded to pain intensity 1, and the most intense color corresponded to intensity 10.

An algorithm was developed to convert the coordinates and intensity of the reports into regions of the body and pain intensity, respectively. After this, the algorithm made the analysis of the progression of the pain based on the reports over a week of work for each subject. Furthermore, it calculated the difference between pain reported in the AM and in the PM to identify if the day of work worsened or was responsible for the aggravation of pain at the end of the day. The results were saved into two CSV files for each subject: one in the format `X_am_pm.csv` and another in the format `X_diff.csv`. The first one contains information regarding the body region with the corresponding pain intensity reported by the subject. The second one contains information regarding the difference between the pain reported in the afternoon and the pain reported in the morning. The algorithm generated also the visual representation of the pain over the body image, where it is possible to identify the differences registered in the `X_diff.csv` (in red if the subject reported more pain in the PM than in the AM, and blue if, after the PM, the pain improved).

A Dashboard was created using streamlit.py [88] to allow the visualization of the results in an easier way so that the analysis of these results would occur faster. The dashboard receives a folder with both CSV format files, two for each subject, and it gets the path to the folder that contains the generated pain images over the week. Then, presents to the user the pain differences reported over the week in an image, but also the tables corresponding to the regions with pain reported and the differences between AM and PM for each day. This is shown in the Figure 4.1. In another tab of the Dashboard, a graphic representation of the pain progression in the different body regions is presented, where the user can choose which body region he wants to observe with the corresponding pain evolution (Figures A.1 and A.2). This Dashboard was fundamental since it was used for the creation of the study groups (control and experimental), allowing an interactive and easy solution for the user to observe the information of each subject.

4.4 Control group vs. Experimental group

With the support of the Dashboard, the Control group (CG) and Experimental group (EG) groups were chosen. Since CSP is the pathology being studied, a region that represents the spine was created, joining three different regions: Neck/Traps (back), Upper Back, and Lower Back. In order to separate healthy from pathological subjects, it was observed via Dashboard if the subject showed pain in any of these regions and if this pain was chronic (existed for at least three months).

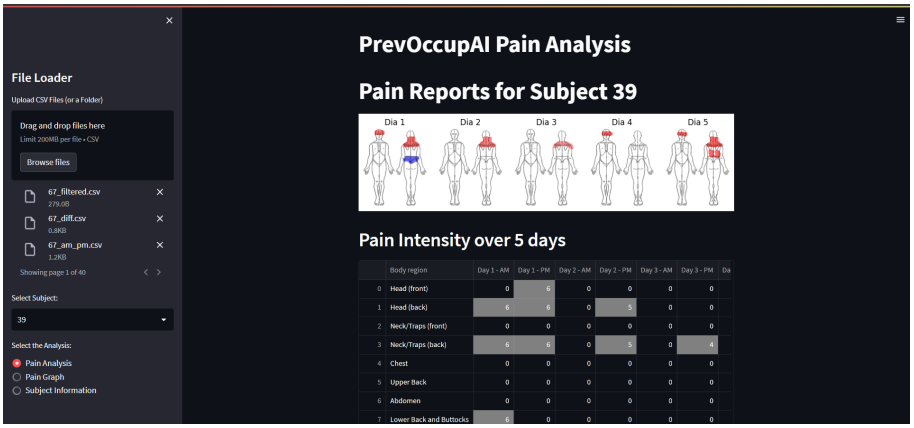

Figure 4.1: Dashboard platform to visualize the pain results.

Table 4.1: Participants statistics.

Variable	CG	EG
Demographic		
Sex (female, %)	60.00	72.70
Age	50.60 (4.51)	54.09 (6.19)
BMI	28.01 (3.64)	27.33 (6.14)
Years of profession	16.80 (9.47)	20.42 (15.18)
Time working per week (hours)	35.50 (3.71)	40.55 (35)
Time sitting per day (week)	7.93 (2.19)	9.27 (3.23)
Time sitting per day (weekend)	3.33 (1.69)	4.26 (1.72)
Physical activity (%)		
Low	40.00	27.30
Moderate	60.00	36.40
High	0.00	36.40

Presented Mean(SD) and percentage.

Table 4.2: Pain Experience.

Variable	Neck	Dorsal	Low Back
Disability (%)			
No inference	27.30	81.80	72.70
Mild	45.50	0.00	18.20
Moderate	27.30	18.20	9.10
Severe	0.00	0.00	0.00
Distress (%)			
No pain-related distress	18.20	72.70	54.50
Mild	63.60	9.10	36.40
Moderate	18.20	18.20	9.10
Severe	0.00	0.00	0.00

Table 4.3: Participants Pain Intensity Statistics.

Intensity	Day 1			Day 3			Day 5		
(0-10)	Neck	Dorsal	Low Back	Neck	Dorsal	Low Back	Neck	Dorsal	Low Back
AM	1.40(2.32)	0.90(1.91)	2.00(2.62)	1.10(1.91)	0.50(1.58)	0.00(0.00)	1.10(1.85)	0.70(1.49)	1.00(1.63)
PM	1.20(2.53)	0.90(2.02)	1.40(2.37)	1.20(1.99)	0.90(2.02)	1.40(2.37)	1.20(2.10)	1.90(2.69)	1.70(2.50)

Presented Mean(SD)

The CG consisted of pain-free participants who had no previous instances of back or lower limb discomfort or injuries that restricted their function or necessitated treatment. The EG comprised individuals who experienced non-specific spinal pain, which means their pain persisted or recurred for a minimum of three months without any identifiable underlying cause [16, 27]. Out of the 40 workers who participated in data collection, 5 were excluded due to experiencing acute spinal pain, 12 were excluded due to missing data, and 7 were excluded as they were outliers that could affect the normality of the data. Consequently, a total of 16 workers participated in the study, with 10 having chronic non-specific spinal pain (EG) and 6 being symptom-free (CG).

To assess the study sample, validated questionnaires and custom-developed questions were employed for characterization. Demographic information such as age (years), gender (female or male), height (centimeters), and mass (kilograms) were collected using a single

questionnaire. The temporal criteria for CSP was established using the ICD-11 (acute < three months; chronic ≥ three months) [27]. The pain severity was evaluated in intensity, distress, and disability components, using three Numeric Pain Rating Scales (NPRS), with a scale of 1 to 10, suggested by ICD11/IASP. Final score categorized these parameters as mild (1-3), moderate (4-6) and severe (7-10) [16]. To evaluate physical activity (PA), the International Physical Activity Questionnaire Short form (IPAQ-SF) [93] was included. This survey comprised seven questions regarding the frequency and duration of vigorous and/or moderate physical activity, walking, and sitting during weekdays. The final score categorized the level of PA as low, medium, or high, along with estimating the weekly PA level in metabolic equivalents. Tables 4.1, 4.2 and 4.3 show the subjects' characteristics.

4.5 Smartphone Sensors and Data Synchronization

To obtain trunk posture data from the subjects, smartphone sensors were chosen as the most fitting equipment. The selection of smartphones was justified by their widespread accessibility and the presence of various sensors within them. Specifically, data from the accelerometer, magnetometer, gyroscope, and rotation vector were collected using a Xiaomi Redmi Note 9, which operates on the Android operating system. It's worth noting that the Android OS limits the sampling rates for accelerometer (ACC), gyroscope (GYR), and rotation vector (RV) data to 100 Hz. In comparison, magnetometer (MAG) data is sampled at 50 Hz. To capture this data, the smartphone was securely positioned on the subject's chest using a harness. For this thesis, only the accelerometer and rotation vector were considered. In Figure 4.4, it is possible to observe the placement of the smartphone for the acquisition as well as the orientation of the axis for this configuration.

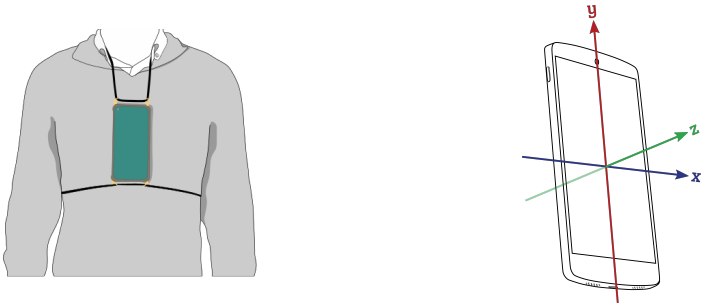

Figure 4.4: Smartphone placement for data acquisition and orientation of the axis.

For devices such as smartphones that run the Android operating system, which is designed to prioritize battery saving, there is a need for intra-device synchronization. However, this prioritization can result in a loss of acquisition priority, leading to sensor data being sampled at different times and with non-equidistant intervals. Consequently, the sensor data from a single device becomes misaligned in time, requiring synchronization. The synchronization process begins by defining the starting and stopping points and then cropping or padding the signals accordingly. For this study, the starting point

is determined as the initial timestamp of the last sensor that began acquiring, and the stopping point is set as the final timestamp of the first sensor that stopped acquiring. Consider the following example where the smartphone sensors start and stop acquisition in the following order:

Start: Accelerometer - Rotation vector

Stop: Accelerometer - Rotation vector

In this scenario, the first sample of the rotation vector would be selected as the starting point and the last sample of the accelerometer as the stopping point. In Figure 4.5, this process is represented. Following the cropping process, each signal must undergo individual resampling to ensure a constant and uniform sampling frequency across all sensors. The SciPy library [86] was employed to generate a new time axis with consistent intervals, beginning and ending at the defined starting and stopping points, respectively. Subsequently, each component of each signal was individually interpolated using the new time axis. This comprehensive approach ensured that the sensors within each device were effectively synchronized.

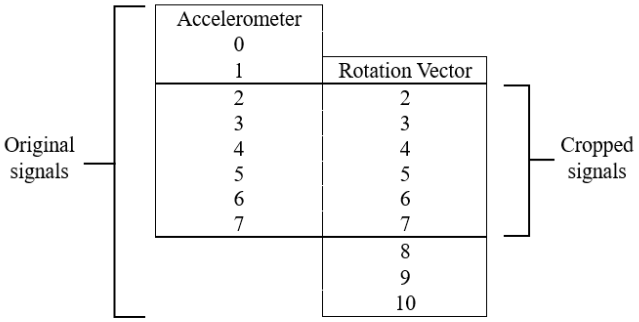

Figure 4.5: Example of signal cropping from the time axis of different smartphone sensors.

4.6 Accelerometer and Rotation Vector Pre-Processing

The accelerometer data was pre-processed through several steps. The first step was the use of a Lowpass filter with a cutoff frequency of 10 Hz. Since gravity has an impact on the accelerometer sensors, influencing the results, this value was removed from the accelerometer axis. After this, the signal was detrended by the removal of its mean value, and smoothing was applied by using a moving average with a window of 150 samples.

The Rotation Vector time series also received a pre-processing with the use of a moving average smoothing filter with a window of 5 samples to eliminate noise. By applying a smoothing filter, the impact of the signal's noise is reduced by averaging out the fluctuations or high-frequency variations in the signal.

For both signals, an algorithm for the creation of windows was developed. This is the result of the need to divide the signals into smaller parts to be analyzed after since the mean time of acquisition for each subject is, approximately, five/six hours (start: 10h30min/11h;

end: 16h30min/17h). To study the pain evolution of the subjects over the working day, the data was separated into morning and afternoon according to the available timestamps. To divide the signal into smaller parts, a window of 15-minutes was chosen. Then, the number of windows created was registered, and the window corresponding to the middle was attributed the tag "L". The window before and after this was also considered as lunch time. This attribution is important since we do not have a ground truth to know for certain when a subject is on a break, but it was assumed that by removing the windows corresponding to the middle of the working shift, the lunch break was being removed. After this, the windows before "L"received the tag "AMx", where x is the window number, and the same happened to the windows after "L", receiving the tag "PMx".

4.7 Algortihm for Detection of Non-seated Intervals

What is being studied is the postural sway of a subject during working hours. The subjects were aware of the goals of the study, and it was explained to them that the seated position while working was the one wanted. Even though this was explained in real data, an assumption that the subject stood up during acquisitions has to be made. So, there is a need to remove the periods where a subject was not seated or their posture transitioned to another. An algorithm to remove this transition between postures and walking periods was developed based on a calculated threshold. This algorithm used the data from the accelerometer to identify the transition between postures and walking intervals. With the accelerometer data in 3-axis (x,y, and z), the acceleration magnitude was calculated:

$$\text{mag} = \sqrt{x_{\text{acc}}^2 + y_{\text{acc}}^2 + z_{\text{acc}}^2} \tag{4.1}$$

Human acceleration during walking and running is well studied in the literature [94]. Satkunskiene et al. [94] study acquired the human body acceleration for different velocities. A threshold for the removal of not-seated periods was calculated based on that study. To approximate the conditions of this thesis, a velocity of 0.55 m/s was considered, describing the walking velocity in a working environment. In the study, the values for the acceleration in x, y, and z coordinates were registered for an accelerometer placed in the C7 vertebrae (closest to the one used in this thesis - sternum), and these values were used to calculate the acceleration magnitude threshold for distinguishing walking periods by ($a_x = 1,02\,\text{m/s}^2$; $a_y = 1,15\,\text{m/s}^2$; $a_z = 1,41\,\text{m/s}^2$):

$$\text{mag} = \sqrt{1.02^2 + 1.15^2 + 1.41^2} \iff \text{mag} = 2.08\,(m/s^2) \tag{4.2}$$

From this equation, we conclude that, approximately, 2 m/s^2 is the threshold that differentiates acceleration magnitude postural changes and walking intervals from seated working periods, during a work shift. A literature reference was found that defines the relationship between energy consumption (metabolic equivalent) during a specific task and acceleration magnitude [95]. For the specific goal of the algorithm, the metabolic equivalent

in occupational situations regarding walking, gathering things at work (encompassing the movement considered as postural transitions), and getting ready to leave is equal to 3 MET [96]. Following the equation described in the literature [95], adapted for this study, the acceleration magnitude threshold was calculated:

$$\text{MET} = 5.289 * acc_{mag} - 8.5548 \iff acc_{mag} = \frac{3 + 8.5548}{5.289} \iff acc_{mag} \approx 2\,(m/s^2) \quad (4.3)$$

Both approaches yielded a similar approximate value for the acceleration magnitude threshold: 2 m/s^2. This was the threshold defined for non-seated interval detection. Consequently, the algorithm removed signal intervals exceeding this threshold, preserving only the portions containing the postural sway data for analysis. Figure 4.6 shows the algorithm working.

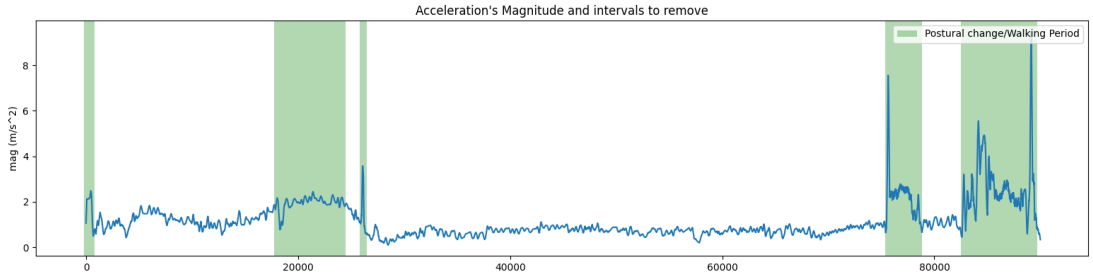

Figure 4.6: Algorithm with the walking periods and postural changes intervals identified.

4.8 Creation of the Dataset for Postural Sway Analysis

Quaternions derived from the Rotation Vector were used to estimate the COP projection in the xy plane. From the previous algorithm, having identified the intervals to be removed, their corresponding indexes are registered. Since the data is synchronized, the removal of these intervals by their indexes is applied to the rotation vector signal, cleaning the signal of non-seated periods and transitions between postures. After this, the quaternions were converted to Euler angles using the SciPy library [86]. The median of each Euler angle was removed in order to center in the origin (coordinate equal to (0,0)) the reference position to be analyzed. The Euler angles were transformed into positions in the xz-plane (according to Figure 4.4), that correspond to the horizontal plane since the subject had the smartphone placed over the chest. This will give the COP projection in this plane that represents the displacement, in millimeters, of the subject while working. This displacement is determined based on the corresponding angle values and distance from the initial position. Figure 4.7 is a representation of how these values are calculated. Assuming the height, h, from the base to the phone, is equal to 0,49 m:

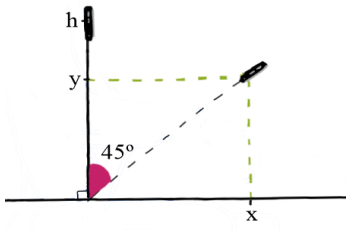

Figure 4.7: Projection decomposition.

$$\begin{cases} x &= h\sin(45°) \\ y &= h\cos(45°) \end{cases} \iff \begin{cases} x &= 0.49\sin(45°) \\ y &= 0.49\cos(45°) \end{cases} \iff \begin{cases} x &= 0.35\,(\text{m}) \\ y &= 0.35\,(\text{m}) \end{cases} \tag{4.4}$$

The COP projection is then calculated for each 15-minute window for each subject. This projection has x and y coordinates, corresponding to the AP and ML directions, respectively. The plot of these coordinates gives us the COP projection of a subject, as seen in Figure's 4.8 first three plots (AP, ML, and the two together, respectively). Taking into account that this study focuses only on the signal that corresponds to the Postural Sway, there is a need to create a limited zone of movement considered Postural Sway. The range for Postural Sway in both AP and ML directions are defined in the literature [97]. For the postural sway analysis, only the signal sections that were inside the ellipse were considered. All other signal sections were removed (AP radius = 25 mm; ML radius = 18 mm). Figure' 4.8 last plot shows the ellipse and only the signal to be analyzed.

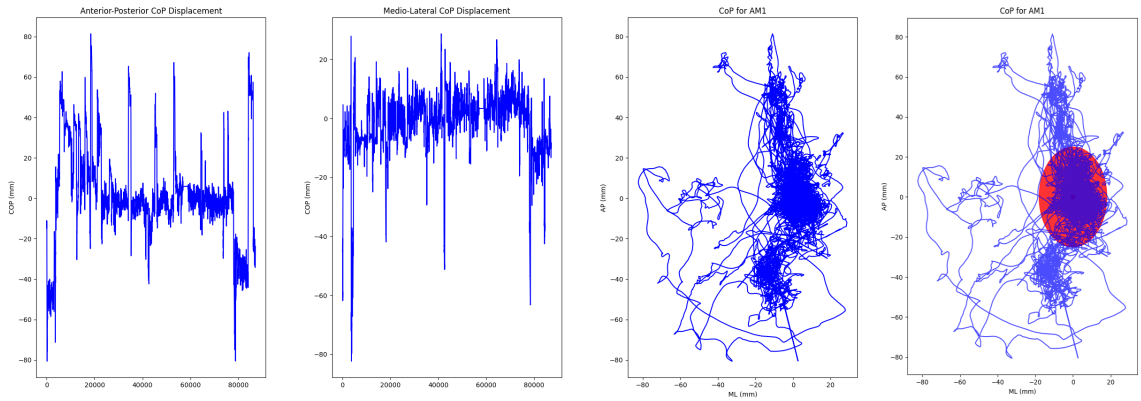

Figure 4.8: COP projection over a 15-minute window, for the day 3 of subject 58.

This ensures that only the signal within the ellipse is retained. The three largest signal segments are saved into a dataframe. The same procedure is repeated for all windows in a day for each subject. The three largest series for both morning (AM) and afternoon (PM) are then selected, creating a dataframe for one subject's day. Application of nonlinear measures requires all series to have the same length across each of the three biggest windows for AM (AM1, AM2, AM3) and PM (PM1, PM2, PM3) COP series. The minimum length among all subjects of the AM COP series is determined, and time series are cropped, saving the first samples until the new length is equal to the minimum previously determined. This ensures that the phenomenon to study is present in all the time series since the initial conditions (signal is recorded when it is inside the ellipse) are maintained. The new size is adopted. The same line of thought is applied to AM2, AM3, PM1, PM2, PM3 COP series. The new series length can be found in Table 4.4. The data is aggregated for each subject across the five working days. A final dataframe is created with all series with the same length, which is later utilized for linear and nonlinear analysis of the extracted data. A schematic of this process is presented in Figure A.3 in the Appendix.

Table 4.4: New COP series lengths for each window.

Window	Length
AM1	1289
AM2	1167
AM3	1171
PM1	1589
PM2	1126
PM3	1246

Table 4.5: Linear parameters of the time series calculated using TSFEL. Adapted from [89]

Parameter	Description
Statistical Domain	
Maximum	Computes the maximum value of the signal.
Minimum	Computes the minimum value of the signal.
Mean	Computes the mean value of the signal.
Standard deviation	Computes the SD of the signal.
Median	Computes the median of the signal.
Root mean square	Computes the RMS of the signal.
Interquartile range	Computes the IQR of the signal.
Variance	Computes the variance of the signal.
Temporal Domain	
Autocorrelation	Computes the autocorrelation of the signal.
Signal distance	Computes the time series traveled distance.

4.9 Linear Parameters

After creating the final dataset containing the COP time series, the extraction of linear measures and nonlinear measures was performed to quantify the amount (linear) and structure (nonlinear) of postural variability for each participant [55]. This was accomplished through two approaches:

1. Linear parameters calculated using the TSFEL Python package: The TSFEL library [89] was employed to facilitate metric calculation. Table 4.5 provides a comprehensive list of the metrics considered in this analysis, along with their interpretations when applied to COP time series data.

2. Parameters related to the characteristics of Postural Sway: Specific parameters related to Postural Sway were also calculated. Table 4.6 presents these parameters, including their units and the formulas used for their calculation [98, 99].

4.10 Nonlinear parameters

Regarding the Nonlinear parameters, these are the ones to study the complexity of the variability. For this study, two Nonlinear measures were calculated:

1. Hurst exponent for q-order of -5, 0, 2 and 4.5, Total width, Positive width, Negative width, and Maximum spectrum calculated by MFDFA analysis using the fathon pyhton library [90].

2. SampEn using the EntropyHub python library [91].

Table 4.6: Linear metrics calculated for Sway analysis [99].

Metric	Formula	Units
Sway area	$\sum_n \lvert X_{n+1} \cdot Y_n - X_n \cdot Y_{n+1} \rvert$	mm^2
Sway range	$\sqrt{(max(X) - min(X))^2 + (max(Y) - min(Y))^2}$	mm
Sway range (AP)	$\lvert max(X) - min(X) \rvert$	mm
Sway range (ML)	$\lvert max(Y) - min(Y) \rvert$	mm
Sway path	$\sum_n \sqrt{(X_{n+1} - X_n)^2 + (Y_{n+1} - Y_n)^2}$	mm
Sway distance (RMS0)	$\sqrt{\frac{1}{N} \sum_n (X^2 + Y^2)}$	mm
Sway velocity	$\frac{fs}{N} \sum_n \sqrt{(X_{n+1} - X_n)^2 + (Y_{n+1} - Y_n)^2}$	mm/s

Table 4.7: Nonlinear parameters calculated using MFDFA.

Parameter	Description
$H_{qs=-5}$	Computes H for q-order = -5.
$H_{qs=0}$	Computes H for q-order = 0.
$H_{qs=2}$	Computes H for q-order = 2.
$H_{qs=4.5}$	Computes H for q-order = 4.5.
Total width	Computes the width of multifractal spectrum.
Positive width	Computes the left width of the multifractal spectrum.
Negative width	Computes the right width of the multifractal spectrum.
Maximum spectrum	Computes maximum value of the multifractal spectrum.

4.10.1 Calculating the Hurst Exponent

While traditional DFA considers just one scaling exponent (equivalent to the Hurst exponent), thus, monofractality, MFDFA begins from the principle that a time series has both small and large oscillations containing relevant information. A q-order range between -5 and 5 was used with a polynomial order of 0.5 (Figure 4.9a). A vector of scaling windows raging between 5 and the length of the time series over 8, with linear ranged steps to achieve 30 windows. The H, a statistical measure that characterizes the long-range dependence or self-similarity of a time series signal, and multifractal spectrogram were calculated (Table 4.7). Figure 4.9b shows a representation of the multifractal spectrogram and the metrics calculated with it.

Since we are considering a multifractal analysis, surrogate data testing is a fundamental component of this method, as it allows for reliable statistical analysis to guarantee that the observed results are not accidental, but are a genuine characteristic of the system. The surrogate data technique involves comparing the distribution of a specific characteristic of the data (known as a discriminating statistic) to the distribution of a subset of the same characteristic calculated in a collection of constructed signals (surrogates) that correspond to the original data set, but do not contain the property being tested [54].

Aligned with this technique, the first step was to compute the surrogates for the COP series that is being analyzed. To compute these surrogates, the Iterated Amplitude Adjusted Fourier Time-series Surrogates (IAAFT) method was used [100].

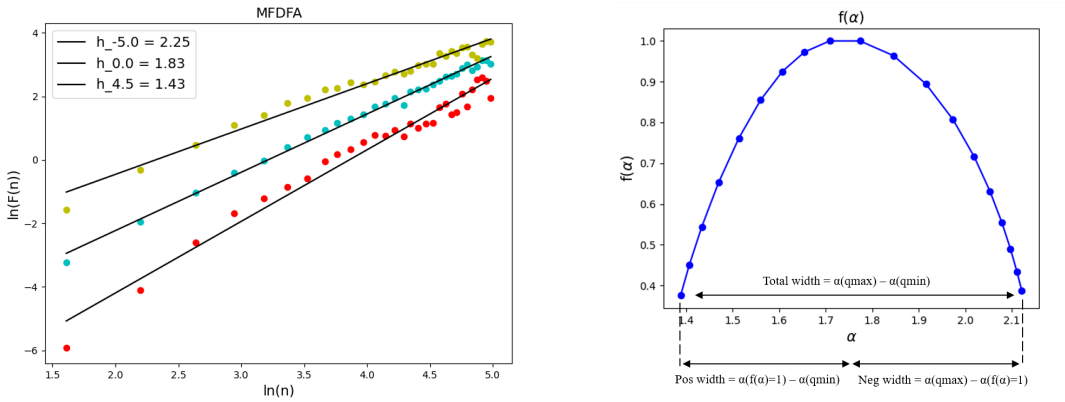

(a) MFDFA plot of the H values.

(b) Multifractal spectrum.

Figure 4.9: MFDFA results.

Following what is described in the literature, and considering the high computational power required as a limitation, the minimum value of 100 surrogates was considered [54]. The following step calculated the list of H, the q-orders, and the multifractal spectrum for all the time series (original COP and 3 x 2 (morning and afternoon) x 3 days surrogates). After this, a q-order equal to 2 is chosen to extract the H values since it is the order used in the traditional detrended fluctuation analysis. If the calculated H for q-order = 2 is greater than 0.5, it indicates that there is a positive correlation between fluctuations at different scales, which suggests that larger fluctuations tend to be followed by other larger fluctuations, and smaller fluctuations tend to be followed by smaller fluctuations, implying a form of persistence or trending behavior in the time series. Having the H values for q-order = 2, the mean and SD of the surrogates' H exponent is computed, and a limit interval is created, where inferior limit (li) and superior limit (ls):

$$\begin{cases} l_i & = mean(H_{surr}) - 2 \cdot std(H_{surr}) \\ l_s & = mean(H_{surr}) + 2 \cdot std(H_{surr}) \end{cases} \tag{4.5}$$

This limit interval is what makes it possible to confirm or reject the Null Hypothesis. If the Null Hypothesis is rejected, then the original COP time series contains genuine fractal characteristics that are not present in the surrogate data. A comparison is then made to check if the H exponent for the original COP time series is inside the limit interval obtained from the surrogates. Figure 4.10 shows an example of both possible outcomes. This procedure was applied to all the original COP time series in their AP and ML planes. Results show that approximately, 81% of the H values for the original time-series are outside this limit interval, and 19% are inside this limit. Therefore, the majority of the data rejects the null hypothesis, confirming that the original time series contains genuine fractal characteristics that cannot be found in the surrogate data.

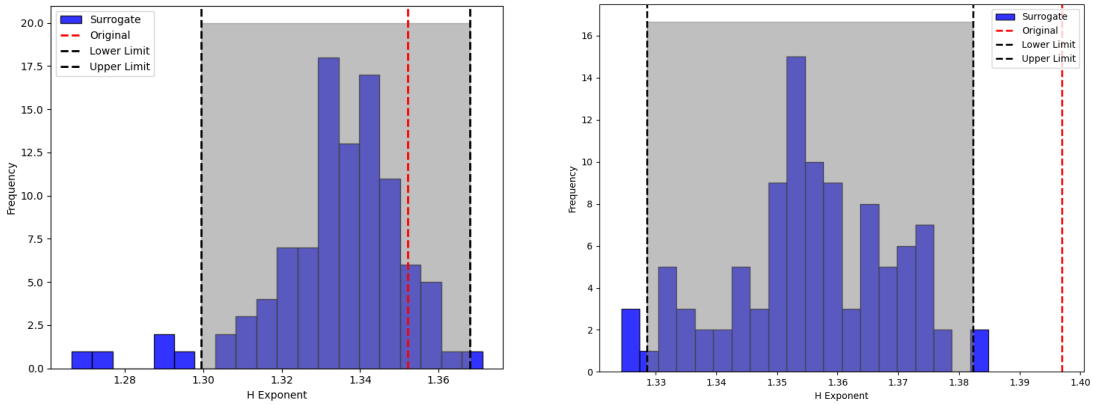

(a) Original value inside the limit interval. (b) Original value outside the limit interval.

Figure 4.10: Result example for checking if the original H value is inside the limit interval.

4.10.2 Calculating the Sample Entropy

SampEn is a nonlinear measure to quantify the regularity or unpredictability of time series data. A higher SampEn value indicates greater irregularity or complexity, suggesting that the time series is less predictable or more disordered. Like the Hurst Exponent, SampEn was calculated for the original time series and surrogates. The SampEn was calculated using an embedded dimension of 4, as recommended in the literature [101]. After calculating the SampEn for the original time series and for all the surrogates, the results show that, approximately, 98% of the original data finds itself outside the limit interval, and only 2% inside this interval. Once again, the majority of the data rejects the null hypothesis, and the time series contains a genuine fractal behavior that is not present in the surrogate data.

4.11 Statistical Analysis

Descriptive statistics were employed to characterize the numerical variables, namely Mean and SD, since the data followed a normal distribution. To assess the distribution of quantitative data, the Shapiro-Wilk test was employed (n=16 < 30). Independent group comparisons were conducted using the Two-way repeated-measures ANOVA for numerical variables if they exhibited a normal distribution. Skewness and kurtosis were also investigated in the case of non-normal distributions for values up to 2.

A two-way repeated measures ANOVA (days and periods of the day over the week vs. group) was used to compare the mean group values of all the calculated linear and nonlinear variables, postural sway parameters, and COP time series characteristics. In instances where there was a significant difference within or between groups ($p < 0.05$), the Bonferroni multiple comparison test was utilized to determine the location of the significant differences, as appropriate.

Chapter 5

Results

5.1 Linear measures

Table B.1 presents the results of the 27 linear metrics that were calculated from the COP time series consisting solely of the postural sway. The two-way repeated-measures ANOVA results for the metrics that reported statistically significant differences are reported in Table B.2, while those that showed no differences are presented in Table B.3. The evolution over time of the metrics that presented statistically significant differences, calculated for the day and week of work for both CG and EG, is shown in Figure 5.1. Similarly, Figures B.1 and B.2 present the same evolution for the metrics without statistically significant differences in inter- or intra-groups.

Amongst all measures, 29.6% of the variables (Maximum ML, Minimum AP, SD AP, Variance AP, RMS ML, IQR AP, and Signal distance AP and ML) demonstrated significant differences either between or within groups. All of its values were higher in the EG.

No significant differences were observed in the postural sway linear metrics within or between groups, as shown in Table B.3 (Sway range AP: $F_{5,70}$=0.720, p=0.611, ${n_p}^2$=0.049; $F_{1,14}$=1.070, p=0.318, ${n_p}^2$=0.071; Sway range ML: $F_{5,70}$=0.839, p=0.527, ${n_p}^2$=0.057; $F_{1,14}$=1.790, p=0.202, ${n_p}^2$=0.113; Sway range:$F_{5,70}$=0.786, p=0.563, ${n_p}^2$=0.053; $F_{1,14}$=1.788, p=0.203, ${n_p}^2$=0.113; Sway distance: $F_{5,70}$=0.370, p=0.868, ${n_p}^2$=0.026; $F_{1,14}$=0.412, p=0.531, ${n_p}^2$=0.029; Sway area: $F_{5,70}$=1.100, p=0.368, ${n_p}^2$=0.073; $F_{1,14}$=0.277, p=0.607, ${n_p}^2$=0.0.019; Sway path: $F_{5,70}$=0.979, p=0.437, ${n_p}^2$=0.065; $F_{1,14}$=0.548, p=0.471, ${n_p}^2$=0.038; Sway velocity: $F_{5,70}$=0.613, p=0.690, ${n_p}^2$=0.042; $F_{1,14}$=0.546, p=0.472, ${n_p}^2$=0.038).

From the 12 metrics calculated from the COP time series, observing the graphs in Figures B.1 and B.2, 58.3% presented tendencies (SD ML, IQR ML, Maximum AP, Autocorrelation AP and ML, Minimum ML and Variance ML) while 41.7% did not (Mean AP, Mean ML, RMS AP, Median AP, and Median ML).

5.1.1 Intra-groups Analysis

From the linear variables that have statistical differences within groups, Maximum ML showed a significant effect between the days of the week ($F_{5,70}$=2.457, p=0.041, ${n_p}^2$=0.149), in particular between the end of Monday and the beginning of Wednesday (p_{bonf}=0.031). No significant effect was verified when comparing between CSP and healthy subjects ($F_{1,14}$=2.951, p=0.108, ${n_p}^2$=0.174). Analyzing the graph for this metric, in Figure 5.1, a decrease was observed as the week progressed for the CG, and higher values for CSP subjects were identified. Furthermore, for both AP and ML components of Signal distance, no significant differences were found between CSP and No CSP subjects (AP: $F_{1,14}$=3.300, p=0.091, ${n_p}^2$=0.191; ML: $F_{1,14}$=3.228, p=0.094, ${n_p}^2$=0.187). However, a significant effect was found between the days of the week (AP: $F_{2.023,28.323}$=8.586, p=0.001, ${n_p}^2$=0.380; ML: $F_{2.011,28.15}$=8.708, p=0.001, ${n_p}^2$=0.383). As Monday progresses, an increase is observed (AP: p_{bonf}=0.032; ML: p_{bonf}=0.035). For Wednesday (AP: p_{bonf}=0.012; ML: p_{bonf}=0.009) and Friday (AP: p_{bonf}=0.002; ML: p_{bonf}=0.002), the same behavior is observed. Furthermore, more significant effects were identified, namely between Monday AM and Wednesday PM (AP: p_{bonf}<0.001; ML: p_{bonf}<0.001), Monday PM and Friday AM (AP: p_{bonf}<0.001; ML: p_{bonf}<0.001), Wednesday AM and Friday AM (AP: p_{bonf}=0.016; ML: p_{bonf}=0.012), and Wednesday PM and Friday AM (AP: p_{bonf}=0.002; ML: p_{bonf}=0.002). The evolution graph in Figure 5.1 shows an increase in the values as the day progresses. Table 5.1 presents a summary of the observed results.

5.1.2 Inter-groups Analysis

Minimum AP showed a significant effect between CSP and No CSP subjects ($F_{1,14}$=8.812, p=0.010, ${n_p}^2$=0.386) and no effect between the days of the week ($F_{5,70}$=1.886, p=0.108, ${n_p}^2$=0.119). By analyzing the corresponding graph in Figure 5.1, a decrease is observed as the week progresses for both CG and EG. CSP office workers presented higher values for the Minimum AP. RMS ML shows the same behavior, with a significant effect between groups ($F_{1,14}$=16.506, p=0.010, ${n_p}^2$=0.388) and no effect between the days of the week ($F_{5,70}$=0.365, p=0.871, ${n_p}^2$=0.025). SD AP is another metric that presents significant differences between CSP and healthy office workers ($F_{1,14}$=8.812, p=0.010, ${n_p}^2$=0.386), in particular between Friday PM values (p_{bonf}=0.030). For the CG, a decrease over the progression of the week is observed in the evolution graph (Figure 5.1). CSP office workers show higher values. IQR AP presents the same behavior with significant differences between groups ($F_{1,14}$=9262, p=0.009, ${n_p}^2$=0.398), showing also a decrease for CG as the week progresses. No effect is observed between the days of the week ($F_{5,70}$=1.431, p=0.224, ${n_p}^2$=0.093). Furthermore, Variance AP has presented significant differences between CSP and No CSP subjects ($F_{1,14}$=14.310, p=0.002, ${n_p}^2$=0.505) and a decrease as the week progresses for the CG can be observed in its evolution graph on Figure 5.1. In addition, no effect is observed between the days of the week ($F_{5,70}$=1.287, p=0.279, ${n_p}^2$=0.084). CSP office workers show higher values. Table 5.2 presents a summary of the results.

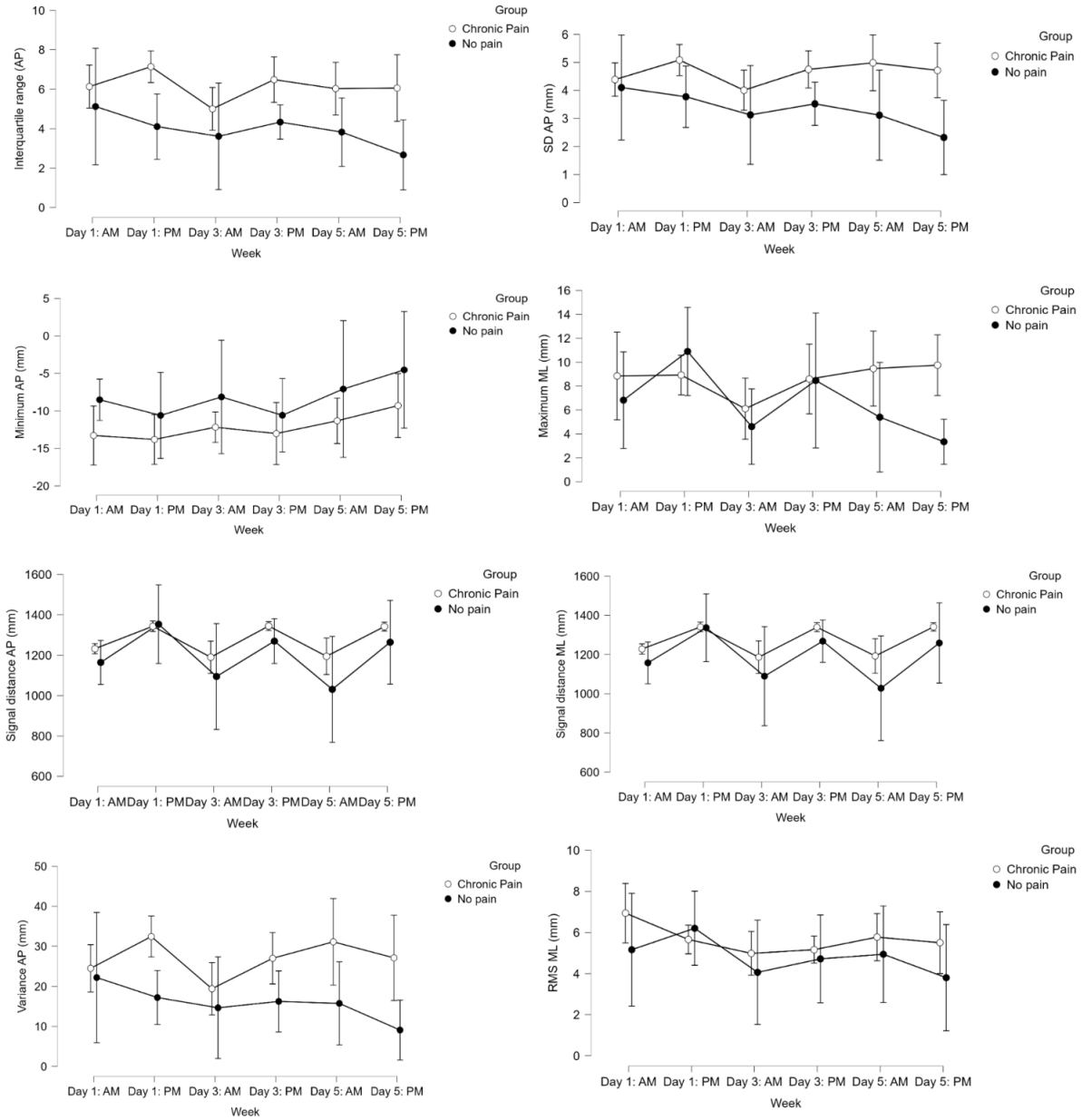

Figure 5.1: Metrics evolution over the day and week for the ones with statistical significance.

5.2 Nonlinear measures

Table C.1 shows the results of the 18 nonlinear metrics calculated from the COP time series containing only the postural sway signal. Table C.2 reports the two-way repeated-measures ANOVA results for metrics that reported statistically significant differences and in Table C.3, the same results for those that showed no differences. Figure 5.2 presents the evolution of the metrics that presented significant differences calculated for the day and week of work for both CG and EG. Figures C.1 and C.2 present the same evolution but in regard to metrics without significant differences in inter- or intra-groups.

Amongst all measures, 27.7% of the variables ($H_{qs=-5}$ AP, $H_{qs=0}$ AP, $H_{qs=4.5}$ AP, and Negative width AP and ML) demonstrated significant differences all between groups. All of its values were higher in the EG.

Regarding the 13 variables that showed no statistically significant differences within or between subjects (observed in Tables C.2 and C.3), the analysis of the evolution graphs presented in Figures C.1 and C.2 showed that 91.7% of the metrics presented tendencies ($H_{qs=2}$ AP; $H_{qs=2}$ ML; $H_{qs=-5}$ ML; $H_{qs=0}$ ML; $H_{qs=4.5}$ ML; Total width AP; Total width ML; Positive width AP; Positive width ML; Maximum spectrum AP; Maximum spectrum ML; SampEn AP) while 8.3% did not (SampEn ML).

5.2.1 Inter-groups analysis

$H_{qs=-5}$ AP presented significant effect between CSP and healthy subjects ($F_{1,14}$=5.478, p=0.035, ${n_p}^2$=0.281), but the same did not occur for the days of the week ($F_{1.668,23.359}$=0.707, p=0.479, ${n_p}^2$=0.048). By analyzing the evolution graph of these metrics in Figure 5.2, CSP subjects present a higher value than healthy office workers.

$H_{qs=0}$ AP and $H_{qs=4.5}$ AP presented also significant differences between CSP and No CSP subjects ($F_{1,14}$=4.837, p=0.045, ${n_p}^2$=0.257; $F_{1,14}$=6.548, p=0.023, ${n_p}^2$=0.329) while no effect observed between the days of the week ($F_{2.167,30.344}$=1.651, p=0.207, ${n_p}^2$=0.105; ($F_{2.340,32.762}$=1.651, p=0.204, ${n_p}^2$=0.105). Analyzing the evolution graphs in Figure 5.2, higher values for CSP subjects when compared to healthy ones are observed. For both components of Negative width, AP and ML, no effect is observed between the days of the week (AP: $F_{3.447,48.257}$=0.826, p=0.500, ${n_p}^2$=0.056; ML: $F_{3.023,42.325}$=0.937, p=0.432, ${n_p}^2$=0.063). However, a significant effect is identified between groups (AP: $F_{1,14}$=6.428, p=0.024, ${n_p}^2$=0.315; ML: $F_{1,14}$=6.716, p=0.021, ${n_p}^2$=0.324). The evolution graph of Figure 5.2 suggests an increase for both CG and EG as the week progresses. Furthermore, for the CG, both components show an increase as the day progresses. CSP subjects present higher values than healthy subjects. Values of the H exponent calculated are always bigger than 1.

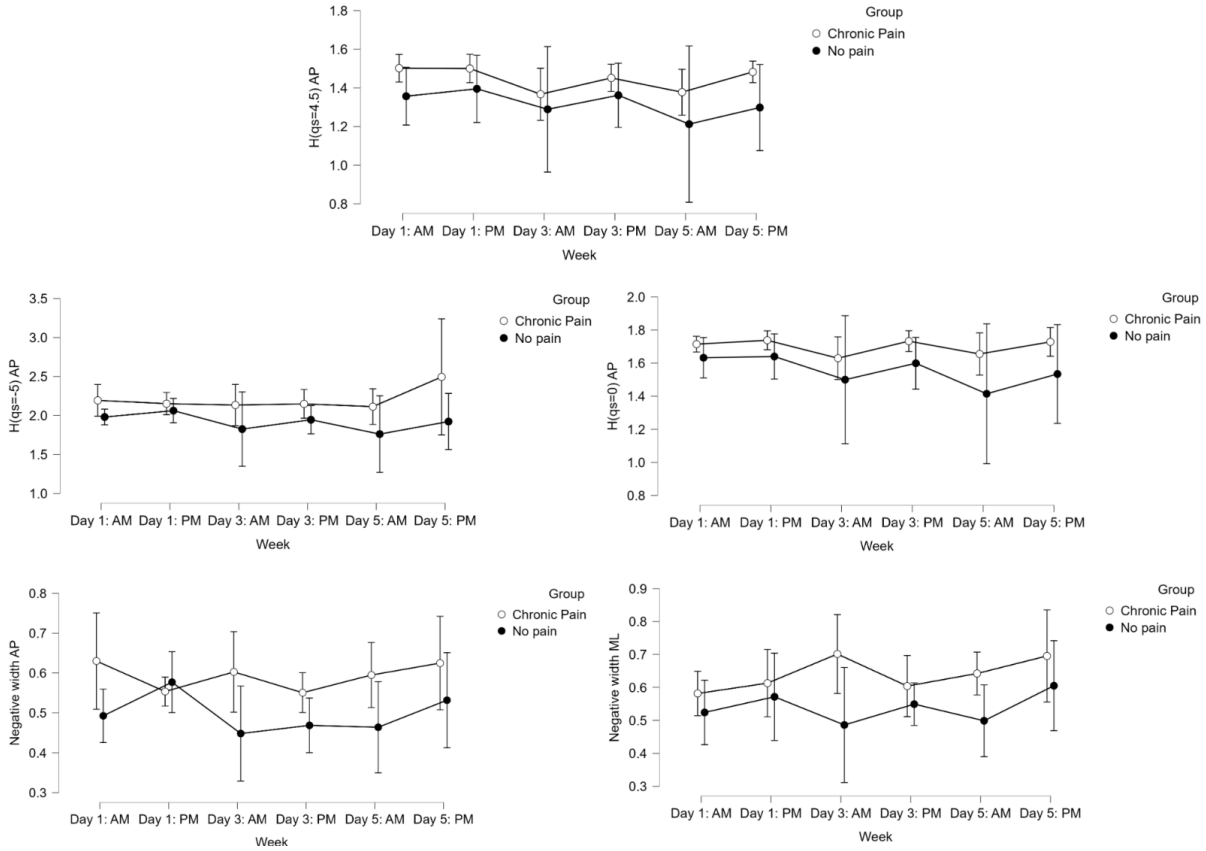

Figure 5.2: Metrics evolution over the day and week for the ones with statistical significance.

Table 5.1: Results of the evolution over day/week of the metrics with statistically significant differences within groups.

		Intra-groups				
		CG		**EG**		
Metric		**Day**	**Week**	**Day**	**Week**	**Values**
Linear metrics						
Maximum	ML	-	Decrease	Increase	-	EG > CG
Signal distance	AP	Increase	-	Increase	-	EG > CG
	ML	Increase	-	Increase	-	EG > CG

5.3 Summary: Observed Results

Table 5.1 presents the differences over the day and week, observed in the calculated metrics that presented statistically significant differences within groups: "Increase"if the metric at the end of the day/week has a higher value than at the beginning of the day/week, "Decrease"if the opposite was observed.

Table 5.2 presents the differences over the day and week observed in the calculated metrics that presented statistically significant differences between groups.

Table 5.2: Results of the evolution over day/week of the metrics with statistically significant differences between groups.

		Inter-groups				
		CG		**EG**		
Metric		**Day**	**Week**	**Day**	**Week**	**Values**
Linear metrics						
Standard deviation	AP	-	Decrease	-	-	EG > CG
Interquartile range	AP	-	Decrease	-	-	EG > CG
Minimum	AP	-	Decrease	-	Decrease	EG > CG
RMS	ML	-	Decrease	-	Decrease	EG > CG
Variance	AP	-	Decrease	-	-	EG > CG
Nonlinear metrics						
$H_{qs=-5}$	AP	-	-	-	-	EG > CG
$H_{qs=0}$	AP	Increase	-	Increase	-	EG > CG
$H_{qs=4.5}$	AP	Increase	-	-	-	EG > CG
Negative width	AP	Increase	Increase	-	Increase	EG > CG
	ML	Increase	Increase	-	Increase	EG > CG

Chapter 6

Discussion

This thesis proposed to analyze and compare the real-time trunk sway oscillations (postural sway) of office workers with and without CSP during work. To achieve this goal, the following hypotheses were tested: (a) Explore the impact of prolonged sitting during work in office workers with and without CSP; (b) Compare the amount of trunk's movement variability between CSP and No CSP office workers, using linear metrics; (c) Compare the complexity of the trunk's movement variability between CSP and no CSP office workers, using nonlinear metrics; (d) Verify if there are changes in the postural sway of both healthy and CSP subjects during the working day/week.

According to this study, there were only a limited number of noteworthy distinctions observed between healthy and CSP office workers, both within and between groups. Even though amongst all linear and nonlinear metrics, several presented tendencies, only a few showed statistically significant differences, making it difficult to find an answer to the defined goals.

From the linear metrics with statistically significant differences that evaluate the amount of trunk's variability in the AP plane (SD AP, IQR AP, Minimum AP, Variance AP), the decreasing of the values presented by both EG and CG subjects suggests that these subjects show a loss of movement variability as the week progresses. Furthermore, in the ML plane, the decrease in the Maximum and RMS values as the week progresses for both CSP and without CSP office workers, suggests that also in the ML plane, there is a loss in the trunk's variability and trunk's variability magnitude, respectively. Signal distance, however, shows an increase in the AP and ML planes for both groups as the day progresses. This suggests that the trunk's variability increases over the day, and that, at the end of the day, the movements are more frequent, and a less static and predictable behavior is identified. In other words, with the progression of the day, office workers show less static behavior, a higher range of movement, and less predictability. As the

week progresses, there seems to be a decrease in the range of movements and an increase in static behavior, along with a loss in trunk variability. This is an indication that during working hours, office workers tend to be more active due to the tasks they are performing, which is also supported by the existing literature [7, 24]. However, as prolonged sitting leads to discomfort, the range of movements reduces, which can be seen in the decrease of variability [23].

Regarding the nonlinear analysis, the values obtained for the different q-orders of the Hurst exponent with MFDFA were always bigger than 1. The Hurst exponent is theoretically defined for values between 0 and 1. A value greater than 1 is not consistent with the original concept of the Hurst exponent, and such a result suggests that MFDFA may not be appropriate for the dataset or that an error might have occurred during the calculation process. In this case, it's not appropriate to make conclusions about the persistence or anti-persistence of the time series based on these values [102]. Even if the metrics show statistically significant differences between CSP and No CSP subjects, the analysis might conclude incorrectly about the characteristics of the complexity of the variability observed. These problems might arise from errors in the data preprocessing and the small size of the time series used in MFDFA analysis. However, the surrogate analysis showed that the original postural sway time series presented multifractal behavior, and the multifractal spectrum that resulted from the MFDFA analysis also corroborates this. Further investigation is imperative in this field as there is a dearth of nonlinear metrics. The chaotic behavior exhibited by postural sway time series could prove to be advantageous in detecting CSP-specific characteristics.

6.1 Conclusions

Prolonged sitting was identified as the second most frequent risk factor emerging in enterprises. In the European Union, workers who typically complete their tasks while seated have a high expression. Office workers are likely to spend more time sitting in their daily work and throughout their professional and personal lives, increasing the risk of occupational diseases, particularly CSP. This can lead to increased discomfort, which can, in turn, affect motor variability.

The main purpose of this thesis was to study the impact of CSP in the Postural Sway pathological subjects when compared to healthy ones, over a week of work, and to explore if Postural Sway can be used as a potential indicator for CSP during computer work tasks. Linear analysis and Nonlinear analysis of the COP time series was conducted, in order to study the amount and complexity of postural sway variability.

Several steps were taken into account to achieve the main objectives. Firstly, data previously acquired with smartphone sensors in the context of the PrevOccupAI project was synchronized and resampled. The signals needed for this study (accelerometer and rotation vector) were subjected to pre-processing (filtering, smoothing, detrending) in order to remove noise. Since the intended data to be analyzed was from office workers

sitting at the desk, an algorithm was developed to remove acquisition periods in which the subjects were not seated, based on a calculated acceleration magnitude threshold. From the COP time series, only the postural's sway corresponding displacement was analyzed.

After applying linear analysis to the COP time series, it was observed that office workers showed an increase in the variability of postural sway throughout the day and a decrease as the week progressed, with CSP subjects showing higher variability values. These results were corroborated by the existing literature. Nevertheless, the metrics obtained from the calculation of postural sway produced inconclusive results.

From the nonlinear analysis, it was observed that the complexity of movement results could not be concluded. This happened because the H exponent values were higher than the theoretically defined range (between 0 and 1), which violated the range and made the results inconclusive for determining the persistence and anti-persistence of the postural sway time series, even though statistically significant differences were identified. However, the multifractal behavior of these time series was corroborated by surrogate analysis and the multifractal spectrum.

Finally, the developed work and obtained results could not give an answer to all the questions that it aspired to, reinforcing the importance and difficulty of studying the postural sway characteristics when comparing CSP and No CSP subjects.

6.2 Limitations

This study's limitations, summarised below, must be considered:

1. Office workers had a smartphone acquiring the data from the beginning through the end of the work shift, resulting in time series with, approximately, 5 hours long. During this time, even though it was explained to the workers that they needed to be seated during the acquisition, and having the lack of ground truth, there is no guarantee that the signal is not contaminated with non-seated periods that need to be removed.

2. The placement of the smartphone over the subject's sternum during the acquisition is also a limitation, since anatomical features may vary between subjects, and the smartphone's axis have their orientation changed.

3. The study sample size is another limitation, mainly in regard to the control group. Of the 40 subjects, only 16 could be analyzed, being the others removed due to missing data and outliers. Only 6 subjects verified the healthy assumption, being a small n for the healthy group.

4. The minimum value referenced in the literature was considered (100 surrogates) since computational power did not allow for surrogate generation to be higher. However, a higher surrogate value is recommended for better results with less error [54].

5. Small length of the postural sway time series extracted with the algorithm using the ellipse to limit the range of movement equivalent to postural sway (in AP and ML directions). This interfered with the results since smaller time series have fewer points, therefore, the results have more oscillation/less information.

6. For the calculation of MFDFA parameters, all signals should have the same length so the postural sway time series were cut. This led to a loss of information that could have the characteristics to be analyzed.

7. MFDFA results for the H exponent values were bigger than 1, violating the theoretically defined interval. This might indicate an error in the pre-processing of the data or that MFDFA is not the best method to analyze the postural sway time series.

6.3 Future work

Following the limitations previously identified, future work should improve study conditions:

1. Since office workers are not seated throughout the entirety of the work shift, future research could investigate the effect of taking breaks over time.

2. Anatomical impact on the smartphone's placement should be taken into account since tilt can be introduced, contaminating the results.

3. A larger number of subjects, especially healthy subjects, must be considered to get less dispersed parameters for the groups.

4. It would be valuable for future research to categorize patients into different severity levels. Soliman, Shousha, and Alayat [103] have demonstrated that the pain intensity is a crucial factor in determining dynamic balance in chronic LBP patients, who exhibit various degrees of impairment in their ability to control dynamic.

5. A different method to analyze the multifractal postural sway time series should be explored.

6. More research is needed to understand how reductions in movement complexity due to aging, injury, and disease affect the adaptability of the movement system and its ability to handle various occupational task conditions.

7. Change Point Detection using a Bayesian approach can be an alternative method suggested by the literature to non-seated interval detection. This approach allows the identification of a change point in time series analysis that could provide more information about the series [104].

8. Machine Learning models to predict the presence of CSP in office workers can be developed based on the linear and nonlinear metrics calculated in this study. Studies already show good results for LBP subjects in this area [19–21].

9. The study of the impacts of fear of movement in the variability and complexity of office workers can be developed since fear of movement causes subjects to restrict and limit their daily activities and social interactions to avoid pain [79].

Bibliography

[1] J. M. Lourenço. *The NOVAthesis LaTeX Template User's Manual*. NOVA University Lisbon. 2021. URL: https://github.com/joaomlourenco/novathesis/raw/main/template.pdf (cit. on p. ii).

[2] W. H. Organization. "Musculoskeletal health". In: *https://www.who.int/news-room/fact-sheets/detail/musculoskeletal-conditions* (2022) (cit. on p. 1).

[3] H. Issever et al. "Depression in tax office workers in Istanbul and its affecting factors". In: *Indoor and Built Environment* 17.5 (2008), pp. 414–420 (cit. on p. 1).

[4] K. Peereboom et al. *Prolonged static sitting at work - Health effects and good practice advice - Executive Summary*. Luxembourg, LUX, 2021 (cit. on pp. 1, 2).

[5] R. Pohling et al. "Work-related factors of presenteeism: The mediating role of mental and physical health." In: *Journal of occupational health psychology* 21.2 (2016), p. 220 (cit. on p. 1).

[6] R. Baker et al. "The short term musculoskeletal and cognitive effects of prolonged sitting during office computer work". In: *International journal of environmental research and public health* 15.8 (2018), p. 1678 (cit. on p. 1).

[7] K. H. Søndergaard et al. "The variability and complexity of sitting postural control are associated with discomfort". In: *Journal of biomechanics* 43.10 (2010), pp. 1997–2001 (cit. on pp. 1, 3, 10, 13, 14, 17, 37).

[8] D. Srinivasan and S. E. Mathiassen. "Motor variability in occupational health and performance". In: *Clinical biomechanics* 27.10 (2012), pp. 979–993 (cit. on p. 1).

[9] A. M. Heredia-Rizo, P. Madeleine, and G. P. Szeto. "Pain mechanisms in computer and smartphone users". In: *Features and Assessments of Pain, Anaesthesia, and Analgesia*. Elsevier, 2022, pp. 291–301 (cit. on pp. 1, 2, 12).

[10] D. Bibbo et al. "A sitting posture monitoring instrument to assess different levels of cognitive engagement". In: *Sensors* 19.3 (2019), p. 455 (cit. on p. 1).

[11] M. L. Ferreira et al. "Global, regional, and national burden of low back pain, 1990–2020, its attributable risk factors, and projections to 2050: a systematic analysis of the Global Burden of Disease Study 2021". In: *The Lancet Rheumatology* 5.6 (2023), e316–e329 (cit. on p. 1).

[12] D. Falla and P. W. Hodges. "Individualized exercise interventions for spinal pain". In: *Exercise and sport sciences reviews* 45.2 (2017), pp. 105–115 (cit. on pp. 1, 2).

[13] A. M. Briggs et al. "Prevalence and associated factors for thoracic spine pain in the adult working population: a literature review". In: *Journal of occupational health* 51.3 (2009), pp. 177–192 (cit. on p. 1).

[14] S. Bevan. "Economic impact of musculoskeletal disorders (MSDs) on work in Europe". In: *Best Practice & Research Clinical Rheumatology* 29.3 (2015), pp. 356–373 (cit. on pp. 1, 2).

[15] I. Ringheim, A. Indahl, and K. Roeleveld. "Reduced muscle activity variability in lumbar extensor muscles during sustained sitting in individuals with chronic low back pain". In: *PLoS One* 14.3 (2019), e0213778 (cit. on p. 2).

[16] R.-D. Treede et al. "Chronic pain as a symptom or a disease: the IASP Classification of Chronic Pain for the International Classification of Diseases (ICD-11)". In: *pain* 160.1 (2019), pp. 19–27 (cit. on pp. 2, 9, 20, 21).

[17] E. Wainwright et al. "Pain, work, and the workplace: a topical review". In: *Pain* 163.3 (2022), pp. 408–414 (cit. on p. 2).

[18] S. D. Tagliaferri et al. "Chronic back pain sub-grouped via psychosocial, brain and physical factors using machine learning". In: *Scientific Reports* 12.1 (2022), p. 15194 (cit. on p. 2).

[19] B. Hu et al. "Using a deep learning network to recognise low back pain in static standing". In: *Ergonomics* 61 (10 2018-10), pp. 1374–1381. ISSN: 13665847. DOI: 10.1080/00140139.2018.1481230 (cit. on pp. 2, 15, 40).

[20] B. X. Liew et al. "Interpretable machine learning models for classifying low back pain status using functional physiological variables". In: *European Spine Journal* 29 (8 2020-08), pp. 1845–1859. ISSN: 14320932. DOI: 10.1007/s00586-020-06356-0 (cit. on pp. 2, 40).

[21] P. Thiry et al. "Machine Learning Identifies Chronic Low Back Pain Patients from an Instrumented Trunk Bending and Return Test". In: *Sensors* 22 (13 2022-07). ISSN: 14248220. DOI: 10.3390/s22135027 (cit. on pp. 2, 15, 16, 40).

[22] E. Oliosi et al. "Week-long Multimodal Data Acquisition of Occupational Risk Factors in Public Administration Workers". In: *2023 19th International Conference on Intelligent Environments (IE)*. 2023, pp. 1–8. DOI: 10.1109/IE57519.2023.10179099 (cit. on pp. 2, 18).

[23] H. Saito et al. "Spinal movement variability associated with low back pain: A scoping review". In: *PLoS ONE* 16 (5 May 2021-05). ISSN: 19326203. DOI: 10.1371/journal.pone.0252141 (cit. on pp. 3, 9, 10, 13, 15–17, 37).

[24] P. Madeleine. "Dynamics of seated computer work before and after prolonged constrained sitting". In: *Journal of applied biomechanics* 28.3 (2012), pp. 297–303 (cit. on pp. 3, 13, 14, 17, 37).

[25] F. Arippa et al. "Postural strategies among office workers during a prolonged sitting bout". In: *Applied ergonomics* 102 (2022), p. 103723 (cit. on p. 3).

[27] S. Perrot et al. "The IASP classification of chronic pain for ICD-11: chronic secondary musculoskeletal pain". In: *Pain* 160.1 (2019), pp. 77–82 (cit. on pp. 4, 20, 21).

[26] J. V. Jacobs, S. M. Henry, and K. J. Nagle. "People With Chronic Low Back Pain Exhibit Decreased Variability in the Timing of Their Anticipatory Postural Adjustments". In: *Behavioral Neuroscience* 123 (2 2009-04), pp. 455–458. ISSN: 07357044. DOI: 10.1037/a0014479 (cit. on p. 4).

[28] C. Larivière et al. "Criterion validity and between-day reliability of an inertial-sensor-based trunk postural stability test during unstable sitting". In: *Journal of Electromyography and Kinesiology* 23 (4 2013-08), pp. 899–907. ISSN: 10506411. DOI: 10.1016/j.jelekin.2013.03.002 (cit. on pp. 4, 15).

[29] N. Bernstein. "The coordination and regulation of movements". In: *(No Title)* (1967) (cit. on p. 4).

[30] M. L. Latash, J. P. Scholz, and G. Schöner. "Motor control strategies revealed in the structure of motor variability". In: *Exercise and sport sciences reviews* 30.1 (2002), pp. 26–31 (cit. on p. 4).

[31] N. Stergiou and L. M. Decker. "Human movement variability, nonlinear dynamics, and pathology: is there a connection?" In: *Human movement science* 30.5 (2011), pp. 869–888 (cit. on pp. 4, 5, 12, 17).

[32] R. T. Harbourne and N. Stergiou. *Movement Variability and the Use of Nonlinear Tools: Principles to Guide Physical Therapist Practice*. 2009, pp. 267–282. URL: http://ptjournal.apta.org/Downloadedfrom (cit. on pp. 4, 5, 10, 12, 16, 17).

[33] J. T. Cavanaugh, D. G. Kelty-Stephen, and N. Stergiou. "Multifractality, interactivity, and the adaptive capacity of the human movement system: a perspective for advancing the conceptual basis of neurologic physical therapy". In: *Journal of neurologic physical therapy: JNPT* 41.4 (2017), p. 245 (cit. on pp. 4, 5, 12).

[34] R. Hedayati et al. "The study of the variability of anticipatory postural adjustments in patients with recurrent non-specific low back pain". In: *Journal of Back and Musculoskeletal Rehabilitation* 27 (1 2014), pp. 33–40. ISSN: 10538127. DOI: 10.3233/BMR-130416 (cit. on pp. 5, 16).

[35] N. Stergiou, Y. Yu, and A. Kyvelidou. "A Perspective on Human Movement Variability With Applications in Infancy Motor Development". In: *Kinesiology Review* 2 (1 2016-08), pp. 93–102. ISSN: 2163-0453. DOI: 10.1123/krj.2.1.93 (cit. on p. 5).

[36] C. Crean, C. Mcgeough, and R. O'Kennedy. "Wearable biosensors for medical applications". In: *Biosensors for Medical Applications* (2012-08), pp. 301–330. DOI: 10.1533/9780857097187.2.301 (cit. on p. 6).

[37] D. K. Shaeffer. "Mems inertial sensors: A tutorial overview". In: *IEEE Communications Magazine* 51 (4 2013), pp. 100–109. DOI: https://doi.org/10.1109/MCOM.2013.6495768 (cit. on pp. 6, 7).

[38] T. Tamura. "Wearable Inertial Sensors and Their Applications". In: *Wearable Sensors: Fundamentals, Implementation and Applications* (2014-09), pp. 85–104. DOI: 10.1016/B978-0-12-418662-0.00024-6 (cit. on pp. 6–8).

[39] M. Kok, J. D. Hol, and T. B. Schön. "Using inertial sensors for position and orientation estimation". In: *Foundations and Trends in Signal Processing* 11 (1-2 2017), pp. 1–153. ISSN: 19328354. DOI: 10.1561/2000000094 (cit. on p. 8).

[40] E. M. Diaz, D. B. Ahmed, and S. Kaiser. "A review of indoor localization methods based on inertial sensors". In: *Geographical and Fingerprinting Data for Positioning and Navigation Systems: Challenges, Experiences and Technology Roadmap* (2018-01), pp. 311–333. DOI: 10.1016/B978-0-12-813189-3.00016-2 (cit. on p. 8).

[41] Android. *Android Open Source Project*. https://source.android.com/devices/sensors/sensor-types?hl=pt-br#rotation_vector (cit. on pp. 8, 9).

[42] D. T. Wade and P. W. Halligan. "The biopsychosocial model of illness: A model whose time has come". In: *Clinical Rehabilitation* 31 (8 2017-08), pp. 995–1004. ISSN: 14770873. DOI: 10.1177/0269215517709890 (cit. on pp. 9, 10).

[43] J. B. Levin et al. *The Relationship Between Self-Efficacy and Disability in Chronic Low Back Pain Patients*. 1996 (cit. on p. 9).

[44] L. G. S. França, P. Montoya, and J. G. V. Miranda. "On multifractals: A non-linear study of actigraphy data". In: *Physica A: Statistical Mechanics and its Applications* 514 (2019-01), pp. 612–619. ISSN: 03784371. DOI: 10.1016/j.physa.2018.09.122 (cit. on pp. 10, 11).

[45] Y.-L. Chen, Y.-C. Chan, and L.-P. Zhang. "Postural Variabilities Associated with the Most Comfortable Sitting Postures: A Preliminary Study". In: *Healthcare* 9 (12 2021-12), p. 1685. ISSN: 2227-9032. DOI: 10.3390/healthcare9121685 (cit. on p. 10).

[46] J. M. Yentes et al. "The appropriate use of approximate entropy and sample entropy with short data sets". In: *Annals of Biomedical Engineering* 41 (2 2013-02), pp. 349–365. ISSN: 15739686. DOI: 10.1007/s10439-012-0668-3 (cit. on p. 10).

[47] Z. Karimi et al. "Determining the interactions between postural variability structure and discomfort development using nonlinear analysis techniques during prolonged standing work". In: *Applied Ergonomics* 96 (2021-10). ISSN: 18729126. DOI: 10.1016/j.apergo.2021.103489 (cit. on p. 10).

[48] A. Emanuelsen et al. "Motor variability in elicited repeated bout rate enhancement is associated with higher sample entropy". In: *Human Movement Science* 68 (2019-12). ISSN: 18727646. DOI: 10.1016/j.humov.2019.102520 (cit. on p. 10).

[49] J. M. Hausdorff. "GAIT DYNAMICS, FRACTALS AND FALLS: FINDING MEANING IN THE STRIDE-TO-STRIDE FLUCTUATIONS OF HUMAN WALKING". In: (2007) (cit. on p. 11).

[50] E. A. Ihlen. "Introduction to multifractal detrended fluctuation analysis in Matlab". In: *Frontiers in Physiology* 3 JUN (2012). ISSN: 1664042X. DOI: 10.3389/fphys.2012.00141 (cit. on p. 11).

[51] H. Stanley et al. "Statistical physics and physiology: Monofractal and multifractal approaches". In: *Physica A* 270 (1999), pp. 309–324. URL: www.elsevier.com/locate/physa (cit. on p. 11).

[52] J. W. Kantelhardt et al. *Multifractal detrended ductuation analysis of nonstationary time series*. 2002, pp. 87–114. URL: www.elsevier.com/locate/physa (cit. on p. 11).

[53] C.-K Peng et al. "Fractal Mechanisms and Heart Rate Dynamics Long-range Correlations and Their Breakdown With Disease". In: *Journal of Electrocardiology* 28 (1995) (cit. on p. 11).

[54] G. Lancaster et al. "Surrogate data for hypothesis testing of physical systems". In: *Physics Reports* 748 (2018-07), pp. 1–60. ISSN: 03701573. DOI: 10.1016/j.physrep.2018.06.001 (cit. on pp. 11, 27, 28, 38).

[55] M. Oliosi et al. "Human movement variability analysis in office-workers: a review". In: *15th International Conference on ICT, Society and Human Beings, ICT 2022, 19th International Conference on Web Based Communities and Social Media, WBC 2022 and 14th International Conference on e-Health, EH 2022 - Held at the 16th Multi Conference on Computer Science and Information Systems, MCCSIS 2022*. IADIS Press, pp. 147–154 (cit. on pp. 12, 26).

[56] A. D. Nordin and J. S. Dufek. "Reviewing the variability-overuse injury hypothesis: Does movement variability relate to landing injuries?" In: *Research Quarterly for Exercise and Sport* 90.2 (2019), pp. 190–205 (cit. on pp. 12, 17).

[57] D. Srinivasan and S. E. Mathiassen. "Motor variability–an important issue in occupational life". In: *Work* 41.Supplement 1 (2012), pp. 2527–2534 (cit. on p. 12).

[58] N. Stergiou. *Nonlinear analysis for human movement variability*. CRC press, 2018 (cit. on pp. 12, 17).

[59] M. Roerdink, P. Hlavackova, and N. Vuillerme. "Center-of-pressure regularity as a marker for attentional investment in postural control: a comparison between sitting and standing postures". In: *Human movement science* 30.2 (2011), pp. 203–212 (cit. on p. 12).

[60] L. Gizzi et al. "People with low back pain show reduced movement complexity during their most active daily tasks". In: *European Journal of Pain* 23.2 (2019), pp. 410–418 (cit. on p. 12).

[61] A. Shahvarpour et al. "Trunk postural balance and low back pain: reliability and relationship with clinical changes following a lumbar stabilization exercise program". In: *Gait & posture* 61 (2018), pp. 375–381 (cit. on p. 12).

[62] A. Longo et al. "Postural reconfiguration and cycle-to-cycle variability in patients with work-related musculoskeletal disorders compared to healthy controls and in relation to pain emerging during a repetitive movement task". In: *Clinical Biomechanics* 54 (2018), pp. 103–110 (cit. on p. 12).

[63] Y. Nishi et al. "Changes in trunk variability and stability of gait in patients with chronic low back pain: Impact of laboratory versus daily-living environments". In: *Journal of Pain Research* (2021), pp. 1675–1686 (cit. on p. 12).

[64] S. Mingels et al. "Lower spinal postural variability during laptop-work in subjects with cervicogenic headache compared to healthy controls". In: *Scientific reports* 11.1 (2021), p. 5159 (cit. on pp. 13, 14).

[65] C. Bontrup et al. "Low back pain and its relationship with sitting behaviour among sedentary office workers". In: *Applied ergonomics* 81 (2019), p. 102894 (cit. on p. 13).

[66] P. Madeleine et al. "Sitting dynamics during computer work are age-dependent". In: *Applied Ergonomics* 93 (2021), p. 103391 (cit. on pp. 14, 17).

[67] A. Ruhe, R. Fejer, and B. Walker. "Does postural sway change in association with manual therapeutic interventions? A review of the literature". In: *Chiropractic and Manual Therapies* 21 (1 2013-02). ISSN: 2045709X. DOI: 10.1186/2045-709X-21-9 (cit. on p. 14).

[68] P. Waongenngarm et al. "Effects of an active break and postural shift intervention on preventing neck and low-back pain among high-risk office workers: A 3-arm cluster-randomized controlled trial". In: *Scandinavian Journal of Work, Environment and Health* 47 (4 2021), pp. 306–317. ISSN: 1795990X. DOI: 10.5271/sjweh.3949 (cit. on p. 14).

[69] S. Voss et al. "Normative database of postural sway measures using inertial sensors in typically developing children and young adults". In: *Gait & posture* 90 (2021), pp. 112–119 (cit. on p. 14).

[70] N. Šarabon, Ž. Kozinc, and G. Marković. "Effects of age, sex and task on postural sway during quiet stance". In: *Gait & Posture* 92 (2022), pp. 60–64 (cit. on p. 15).

[71] T. Vilarinho et al. "A Combined Smartphone and Smartwatch Fall Detection System". In: *2015 IEEE International Conference on Computer and Information Technology; Ubiquitous Computing and Communications; Dependable, Autonomic and Secure Computing; Pervasive Intelligence and Computing* (2015-10), pp. 1443–1448. DOI: 10.1109/CIT/IUCC/DASC/PICOM.2015.216. URL: http://ieeexplore.ieee.org/document/7363260/ (cit. on p. 15).

[72] S. Ayub et al. "Pedestrian direction of movement determination using smartphone". In: 2012, pp. 64–69. ISBN: 9780769548036. DOI: 10.1109/NGMAST.2012.36 (cit. on p. 15).

[73] M. S. Pan and H. W. Lin. "A step counting algorithm for smartphone users: Design and implementation". In: *IEEE Sensors Journal* 15 (4 2015-04), pp. 2296–2305. ISSN: 1530437X. DOI: 10.1109/JSEN.2014.2377193 (cit. on p. 15).

[74] D. Jun et al. "Are measures of postural behavior using motion sensors in seated office workers reliable?" In: *Human factors* 61.7 (2019), pp. 1141–1161 (cit. on p. 15).

[75] K. L. Hsieh and J. J. Sosnoff. "Smartphone accelerometry to assess postural control in individuals with multiple sclerosis". In: *Gait & Posture* 84 (2021), pp. 114–119 (cit. on p. 16).

[76] J. Polechoński et al. "Applicability of smartphone for dynamic postural stability evaluation". In: *BioMed Research International* 2019 (2019) (cit. on p. 16).

[77] C. J. Marshall et al. "Smartphone Technology to Remotely Measure Postural Sway during Double-and Single-Leg Squats in Adults with Femoroacetabular Impingement and Those with No Hip Pain". In: *Sensors* 23.11 (2023), p. 5101 (cit. on p. 16).

[78] K. Pooranawatthanakul and A. Siriphorn. "Comparisons of the validity and reliability of two smartphone placements for balance assessment using an accelerometer-based application". In: *European Journal of Physiotherapy* 22.4 (2020), pp. 236–242 (cit. on p. 16).

[79] J. S. Hamid et al. "Cluster analysis for identifying sub-groups and selecting potential discriminatory variables in human encephalitis". In: *BMC Infectious Diseases* 10 (2010-12). ISSN: 14712334. DOI: 10.1186/1471-2334-10-364 (cit. on pp. 16, 40).

[80] J. M. C. L. E. L. A. J. M. C. L. T. V. P. S. V. Serra et al. *DOR ® Questionários sobre Dor Crónica Volume 15 Nº4/2007*. Escala pcs. 2007 (cit. on p. 16).

[81] Érica Brandão de Moraes Vieira et al. "Self-Efficacy and Fear Avoidance Beliefs in Chronic Low Back Pain Patients: Coexistence and Associated Factors". In: *Pain Management Nursing* 15 (3 2014), pp. 593–602. ISSN: 15249042. DOI: 10.1016/j.pmn.2013.04.004 (cit. on p. 16).

[82] Y. Karasawa et al. "Association between change in self-efficacy and reduction in disability among patients with chronic pain". In: *PLoS ONE* 14 (4 2019-04). ISSN: 19326203. DOI: 10.1371/journal.pone.0215404 (cit. on p. 16).

[83] R. E. Van Emmerik et al. "Comparing dynamical systems concepts and techniques for biomechanical analysis". In: *Journal of sport and health science* 5.1 (2016), pp. 3–13 (cit. on p. 16).

[84] N. M. Lau, C. S. Choy, and D. H. Chow. "Identifying Multifractality Structure on Postural Sway". In: *Journal of Ergonomics* 05 (02 2015). ISSN: 21657556. DOI: 10.4172/2165-7556.1000137 (cit. on p. 17).

[85] C. R. Harris et al. "Array programming with NumPy". In: *Nature* 585 (7825 2020-09), pp. 357–362. ISSN: 14764687. DOI: 10.1038/s41586-020-2649-2 (cit. on p. 18).

[86] P. Virtanen et al. "SciPy 1.0: fundamental algorithms for scientific computing in Python". In: *Nature Methods* 17 (3 2020-03), pp. 261–272. ISSN: 15487105. DOI: 10.1038/s41592-019-0686-2 (cit. on pp. 18, 22, 24).

[87] W. Mckinney. "Data Structures for Statistical Computing in Python". In: (2010) (cit. on p. 18).

[88] A. Treuille, A. Kelly, and T. Teixeira. *Streamlit*. https://docs.streamlit.io/. 2018 (cit. on pp. 18, 19).

[89] M. Barandas et al. "TSFEL: Time Series Feature Extraction Library". In: *SoftwareX* 11 (2020), p. 100456 (cit. on pp. 18, 26).

[90] S. Bianchi. "fathon: A Python package for a fast computation of detrendend fluctuation analysis and related algorithms". In: *Journal of Open Source Software* 5 (45 2020-01), p. 1828. DOI: 10.21105/joss.01828 (cit. on pp. 18, 26).

[91] M. W. Flood and B. Grimm. "EntropyHub: An open-source toolkit for entropic time series analysis". In: *PLoS ONE* 16 (11 November 2021-11). ISSN: 19326203. DOI: 10.1371/journal.pone.0259448 (cit. on pp. 18, 26).

[92] R. D. Treede et al. "Chronic pain as a symptom or a disease: The IASP Classification of Chronic Pain for the International Classification of Diseases (ICD-11)". In: *Pain* 160 (1 2019-01). Numeric Pain Rating Scale, pp. 19–27. ISSN: 18726623. DOI: 10.1097/j.pain.0000000000001384 (cit. on p. 18).

[93] C. L. Craig et al. "International physical activity questionnaire: 12-country reliability and validity." In: *Medicine and science in sports and exercise* 35.8 (2003), pp. 1381–1395 (cit. on p. 21).

[94] D Satkunskiene et al. "487. Acceleration based evaluation of the human walking and running parameters." In: *Journal of Vibroengineering* 11.3 (2009) (cit. on p. 23).

[95] B. Mortazavi et al. "MET calculations from on-body accelerometers for exergaming movements". In: *2013 IEEE International Conference on Body Sensor Networks*. IEEE. 2013, pp. 1–6 (cit. on pp. 23, 24).

[96] B. E. Ainsworth et al. "Compendium of physical activities: an update of activity codes and MET intensities". In: *Medicine and science in sports and exercise* 32.9; SUPP/1 (2000), S498–S504 (cit. on p. 24).

[97] D. Ohlendorf et al. "Standard reference values of the postural control in healthy female adults aged between 31 and 40 years in Germany: an observational study". In: *Journal of Physiological Anthropology* 39 (2020), pp. 1–7 (cit. on p. 25).

[98] V. Agostini et al. "Postural sway in volleyball players". In: *Human Movement Science* 32 (3 2013-06), pp. 445–456. ISSN: 01679457. DOI: 10.1016/j.humov.2013.01.002 (cit. on p. 26).

[99] F. Quijoux et al. "A review of center of pressure (COP) variables to quantify standing balance in elderly people: Algorithms and open-access code". In: *Physiological reports* 9.22 (2021), e15067 (cit. on pp. 26, 27).

[100] M. Group. *IAAFT: Iterative Amplitude Adjusted Fourier Transform*. https://github.com/mlcs/iaaft. GitHub repository. 2021 (cit. on p. 27).

[101] L. Montesinos, R. Castaldo, and L. Pecchia. "On the use of approximate entropy and sample entropy with centre of pressure time-series". In: *Journal of neuroengineering and rehabilitation* 15.1 (2018), pp. 1–15 (cit. on p. 29).

[102] R. F. Ceballos and F. F. Largo. "On The Estimation of the Hurst Exponent Using Adjusted Rescaled Range Analysis, Detrended Fluctuation Analysis and Variance Time Plot: A Case of Exponential Distribution". In: *Imperial Journal of Interdisciplinary Research (IJIR* 3 (2017). ISSN: 2454-1362 (cit. on p. 37).

[103] E. S. Soliman, T. M. Shousha, and M. S. Alayat. "The effect of pain severity on postural stability and dynamic limits of stability in chronic low back pain." In: *Journal of back and musculoskeletal rehabilitation* 30.5 (2017), pp. 1023–1029 (cit. on p. 39).

[104] E. Almeida. "Change Point Detection — A Bayesian Approach". In: (2023). URL: https://towardsdatascience.com/change-point-detection-a-bayesian-approach-8eb3cfca4a6e (cit. on p. 39).

Appendix A

Dashboard and Window creation steps

Figure A.1: Dashboard example with the table for pain differences between days of the week.

Figure A.2: Dashboard example with a graph of pain evolution during the week.

	Window	COP1_size	COP2_size	COP3_size
0	AM1	3500	2100	1200
1	AM2	2800	1300	820
2	AM3	1500	900	750
3	AM4	530	320	200
4	L	2000	1800	1400
5	L	1500	980	750
6	L	3100	1600	1010
7	PM1	5200	3200	2400
8	PM2	2000	1200	860
9	PM3	180	100	73
10	PM4	320	150	90
11	PM5	410	300	140

	Window	COP_pos_x	COP_pos_y	COP_size
0	AM1	[...]	[...]	3500
1	AM2	[...]	[...]	2800
2	AM3	[...]	[...]	1500
3	PM1	[...]	[...]	5200
4	PM2	[...]	[...]	2000
5	PM3	[...]	[...]	3200

A

	Window	COP_pos_x	COP_pos_y	COP_size
0	AM1	[...]	[...]	3500
1	AM2	[...]	[...]	2800
2	AM3	[...]	[...]	1500
3	PM1	[...]	[...]	5200
4	PM2	[...]	[...]	2000
5	PM3	[...]	[...]	3200

B

	Window	COP_pos_x	COP_pos_y	COP_size
0	AM1	[...]	[...]	2100
1	AM2	[...]	[...]	1250
2	AM3	[...]	[...]	2300
3	PM1	[...]	[...]	1100
4	PM2	[...]	[...]	1820
5	PM3	[...]	[...]	1300

C

	Window	COP_pos_x	COP_pos_y	COP_size
0	AM1	[...]	[...]	1280
1	AM2	[...]	[...]	2030
2	AM3	[...]	[...]	3500
3	PM1	[...]	[...]	2400
4	PM2	[...]	[...]	1420
5	PM3	[...]	[...]	1850

A

	Window	COP_pos_x	COP_pos_y	COP_size
0	AM1	[...]	[...]	1280
1	AM2	[...]	[...]	1250
2	AM3	[...]	[...]	1500
3	PM1	[...]	[...]	1100
4	PM2	[...]	[...]	1420
5	PM3	[...]	[...]	1300

B

	Window	COP_pos_x	COP_pos_y	COP_size
0	AM1	[...]	[...]	1280
1	AM2	[...]	[...]	1250
2	AM3	[...]	[...]	1500
3	PM1	[...]	[...]	1100
4	PM2	[...]	[...]	1420
5	PM3	[...]	[...]	1300

C

	Window	COP_pos_x	COP_pos_y	COP_size
0	AM1	[...]	[...]	1280
1	AM2	[...]	[...]	1250
2	AM3	[...]	[...]	1500
3	PM1	[...]	[...]	1100
4	PM2	[...]	[...]	1420
5	PM3	[...]	[...]	1300

Figure A.3: Step-by-step schematic on how to achieve the final COP series.

Appendix B

Linear results

In the next pages are presented:

1. Figures B.1 and B.2: Additional results graphs of the linear metrics without statistically significant differences;
2. Table B.1: Results table for each calculated metric, with the Mean±SD values, and the p-values for the two-way repeated-measures ANOVA between and whiting groups;
3. Tables B.2 and B.3: Results from the two-way repeated-measures ANOVA, all the metrics calculated, presented first the ones with statistically significant differences.

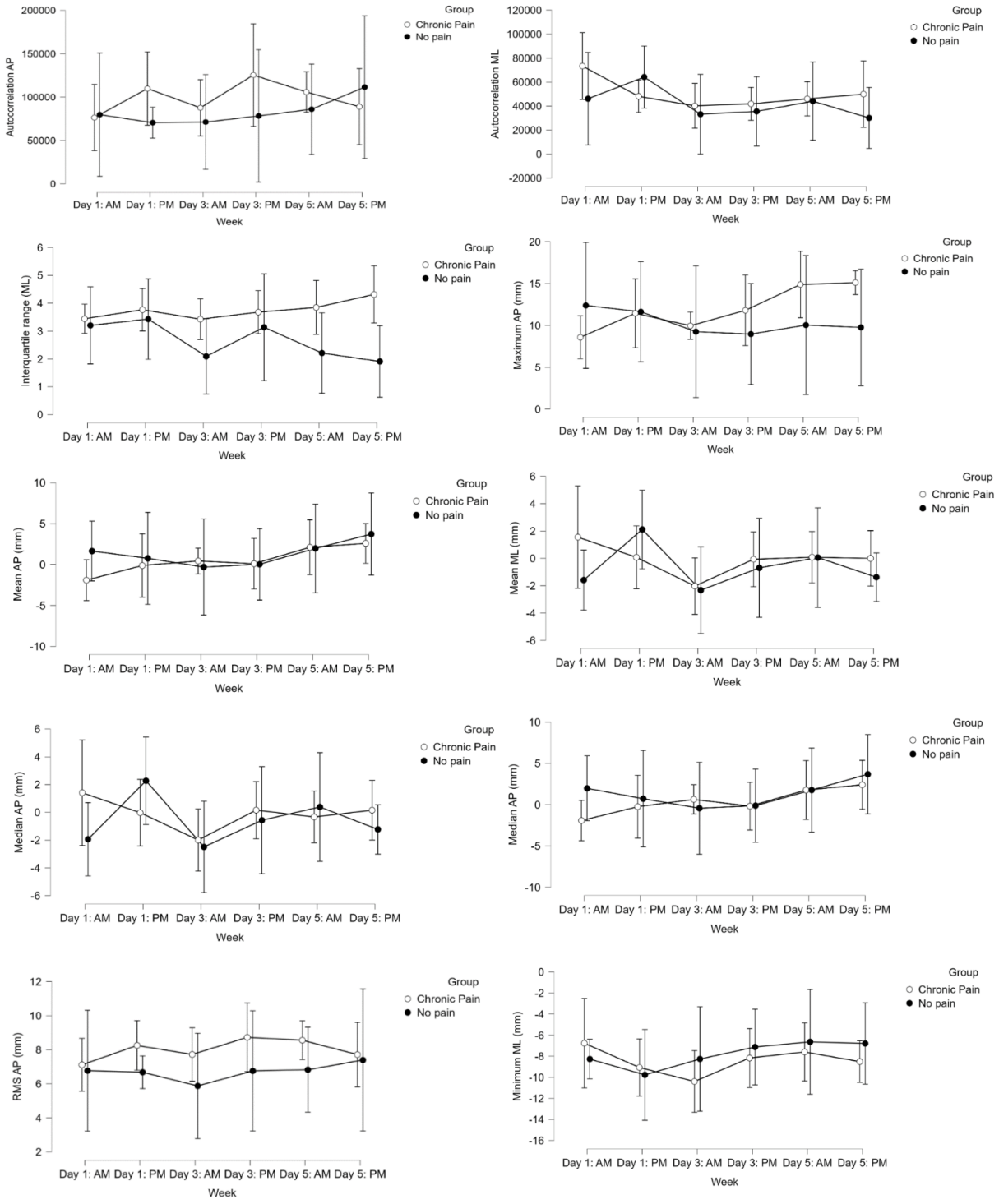

Figure B.1: Linear metrics evolution over the day and week for the ones without statistical significance.

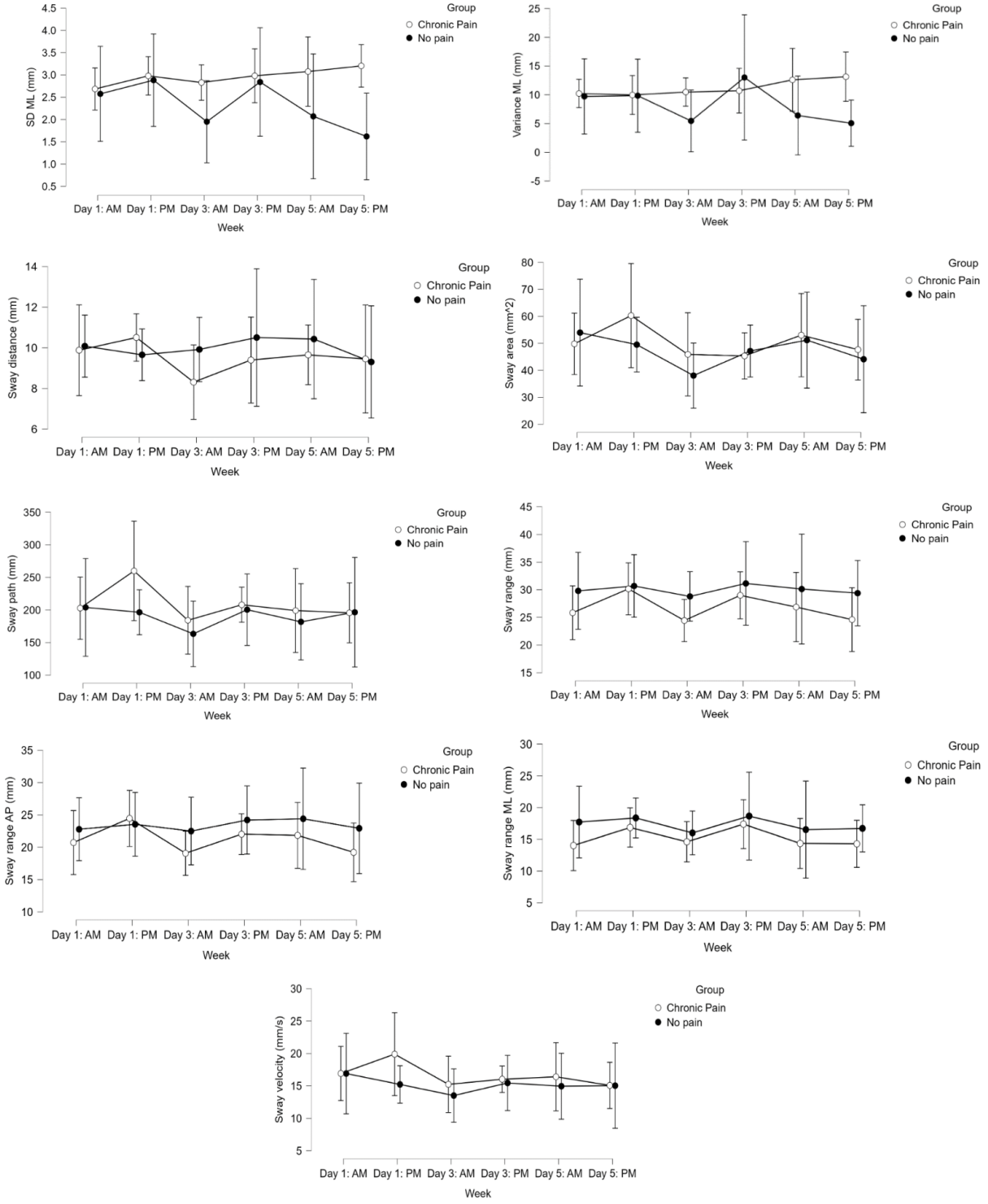

Figure B.2: Linear metrics evolution over the day and week for the ones without statistical significance. (cont.)

Table B.1: Results [Mean±SD] for calculated Linear measures with p-values for within and between subjects comparison.

Metric	Day/Time												WG	BG
	CG						EG						p	p
	Day 1		Day 3		Day 5		Day 1		Day 3		Day 5			
	AM	PM	AM	PM	AM	PM	AM	PM	AM	PM	AM	PM		
Sway area	53.98±25.92	49.52±7.05	38.06±11.54	47.17±6.18	51.20±22.75	44.12±15.94	49.83±18.92	60.29±28.24	45.92±21.45	45.35±14.11	53.04±20.02	47.67±23.14	0.37	0.61
Sway range	29.80±6.26	30.69±3.96	28.80±3.95	31.14±6.23	30.13±10.07	29.39±5.91	25.84±6.55	30.17±6.63	24.44±8.04	29.00±9.58	26.87±8.38	24.60±10.73	0.56	0.20
Sway range (AP)	22.79±3.80	23.55±4.58	22.50±3.58	24.21±3.82	24.41±8.39	22.94±7.23	20.73±6.25	24.47±6.68	19.08±6.66	22.03±8.28	21.84±7.03	19.22±8.70	0.61	0.32
Sway range (ML)	17.73±6.01	18.38±1.76	16.02±3.24	18.67±5.90	16.54±8.03	16.73±5.24	14.03±4.94	16.87±3.63	14.62±5.49	17.40±6.77	14.36±5.79	14.30±6.43	0.53	0.20
Sway path	29.80±6.26	49.52±7.05	28.80±3.95	47.17±6.18	30.13±10.07	44.12±15.94	25.84±6.55	60.29±28.24	24.44±8.04	45.35±14.11	26.87±8.38	47.67±23.14	0.44	0.47
Sway distance	10.09±0.85	9.66±1.38	9.92±1.78	10.51±2.66	10.433±3.58	9.31±2.80	9.88±3.60	10.51±1.42	8.31±3.06	9.40±2.34	9.66±2.24	9.45±4.00	0.87	0.53
Sway velocity	16.90±7.83	15.22±2.20	13.51±3.45	15.45±3.54	14.95±6.16	15.04±5.81	16.91±7.61	19.90±9.30	15.24±6.42	16.02±4.69	16.41±6.67	15.08±6.89	0.69	0.47
Maximum (AP)	12.39±7.66	11.63±2.80	9.26±8.77	8.97±7.59	10.04±6.21	9.77±7.44	8.58±4.65	11.45±4.56	9.97±3.27	11.81±7.24	14.89±4.27	15.12±2.20	0.62	0.24
Maximum (ML)	6.83±3.81	10.90±1.99	4.61±4.15	8.47±6.08	5.40±6.37	3.34±3.20	8.84±5.05	8.92±2.38	6.11±3.62	8.59±4.29	9.47±3.93	9.75±4.46	**0.04***	0.11
Minimum (AP)	-8.51±3.81	-10.60±5.89	-8.14±5.05	-10.58±4.58	-7.07±9.11	-4.52±7.07	-13.28±5.32	-13.81±4.84	-12.18±3.76	-13.02±7.14	-11.32±3.87	-9.29±5.98	0.11	**0.01***
Minimum (ML)	-8.27±1.40	-7.13±4.55	-8.26±4.69	-9.77±3.93	-6.63±3.46	-6.79±4.13	-6.76±6.22	-8.16±3.55	-10.39±4.02	-9.07±3.34	-7.59±4.53	-8.51±2.92	0.46	0.51
Mean (AP)	1.65±4.37	0.76±4.32	-0.30±5.03	0.04±5.25	1.97±5.04	3.73±5.34	-1.90±4.02	-0.12±4.28	0.44±2.94	0.11±5.64	2.11±4.36	2.59±3.37	0.21	0.48
Mean (ML)	-1.59±1.56	2.11±3.50	-2.33±3.04	-0.69±2.48	0.057±3.92	-1.38±2.47	1.55±5.40	0.08±2.82	-2.03±2.50	-0.07±2.48	0.08±2.79	0.00±3.33	0.14	0.44
Standard deviation (AP)	4.10±1.73	3.78±0.89	3.13±2.01	3.52±1.21	3.12±1.33	2.32±1.55	4.39±1.14	5.09±0.81	4.01±0.95	4.75±1.08	4.99±1.58	4.72±1.00	0.22	**0.001***
Standard deviation (ML)	2.58±1.25	2.88±0.64	1.95±1.11	2.84±1.77	2.07±1.18	1.62±1.06	2.68±0.78	2.98±0.39	2.83±0.83	2.98±0.96	3.07±1.22	3.20±1.00	0.38	0.07
Median (AP)	1.98±4.80	0.73±4.52	-0.43±4.63	-0.12±5.39	1.78±4.95	3.69±5.23	-1.92±3.76	-0.24±4.28	0.64±2.92	-0.17±5.38	1.78±4.83	2.41±4.28	0.28	0.45
Median (ML)	-1.94±2.18	2.28±3.74	-2.49±3.21	-0.57±2.63	0.39±4.14	-1.23±2.32	1.41±5.57	-0.02±2.94	-2.00±2.66	0.16±2.43	-0.34±2.81	0.16±3.71	0.17	0.53
Variance (AP)	22.21±13.96	17.22±6.44	14.65±14.41	16.25±9.11	15.75±10.28	9.09±8.98	24.52±11.77	32.45±8.86	19.41±8.22	27.02±11.40	31.13±16.82	27.13±10.41	0.28	**0.002***
Variance (ML)	9.12±8.97	9.85±3.62	5.46±4.45	13.02±14.51	6.40±4.45	5.07±6.29	10.23±5.04	9.97±2.71	10.48±5.58	10.71±6.20	12.60±9.12	13.14±8.41	0.69	0.25
Root mean square (AP)	6.77±3.04	6.68±1.56	5.87±3.63	6.75±2.00	6.82±2.99	7.39±5.14	7.11±2.59	8.25±1.95	7.72±2.34	8.73±2.12	8.56±2.13	7.71±2.21	0.87	0.06
Root mean square (ML)	5.16±2.66	6.20±1.54	4.06±2.27	4.72±1.83	4.94±1.86	3.80±2.25	6.94±2.09	5.66±1.15	4.98±1.65	5.16±0.88	5.77±1.74	5.50±1.68	0.12	**0.01***
Interquartile range (AP)	5.12±2.97	4.11±1.71	3.61±2.99	4.33±1.31	3.83±1.57	2.67±2.34	6.13±2.40	7.14±1.33	5.01±1.93	6.49±1.85	6.03±2.67	6.06±2.24	0.15	**0.009***
Interquartile range (ML)	3.20±1.73	3.43±0.86	2.09±1.50	3.14±2.63	2.21±1.20	1.91±1.44	3.44±1.21	3.77±0.80	3.43±1.55	3.68±1.29	3.85±1.74	4.32±1.95	0.51	0.06
Autocorrelation (AP)[a]	7.98±5.84	7.06±3.06	7.13±6.72	7.83±4.61	8.60±6.29	11.15±10.20	7.64±5.87	10.99±5.75	8.77±4.73	12.54±6.94	10.59±4.46	8.90±5.17	0.80	0.23
Autocorrelation (ML)[a]	4.61±3.48	6.42±2.41	3.32±2.89	3.55±2.41	4.40±3.00	3.01±2.33	7.33±4.05	4.81±2.10	4.02±2.69	4.18±1.80	4.60±2.10	4.99±3.31	0.15	0.13
Signal distance (AP)[b]	11.64±1.62	13.54±0.41	10.95±3.234	12.70±1.69	10.31±3.23	12.64±1.73	12.32±0.18	13.44±0.14	11.90±1.17	13.457±0.14	11.95±1.26	13.42±0.09	**0.001***	0.09
Signal distance (ML)[b]	11.57±1.60	13.37±0.11	10.84±3.22	12.68±1.74	10.28±3.28	12.59±1.70	12.28±0.17	13.41±0.09	11.86±1.23	13.39±0.11	11.93±1.26	13.41±0.11	**0.001***	0.09

Abbreviations WG: Within Group; BG: Between Group; *: indicates $p<0.05$; [a]: $\times 10^4$; [b]: $\times 10^2$

Table B.2: Results from Two-way repeated-measures ANOVA for statistically significant linear measures.

Metrics		**Group**	**Week**	**Week x Group**
Maximum	AP	$F_{1,14}$=1.483	$F_{5,70}$=0.705	$F_{5,70}$=1.505
		p=0.243	p=0.622	p=0.200
		$n_p{}^2$=0.096	$n_p{}^2$=0.048	$n_p{}^2$=0.097
	ML	$F_{1,14}$=2.951	$F_{5,70}$**=2.457**	$F_{5,70}$=2.141
		p=0.108	**p=0.041**	p=0.070
		$n_p{}^2$=0.174	$n_p{}^2$**=0.149**	$n_p{}^2$=0.133
Minimum	AP	$F_{1,14}$**=8.812**	$F_{5,70}$=1.886	$F_{5,70}$=0.107
		p=0.010	p=0.108	p=0.991
		$n_p{}^2$**=0.386**	$n_p{}^2$=0.119	$n_p{}^2$=0.008
	ML	$F_{1,14}$=0.451	$F_{3.592,50,282}$=0.902	$F_{3.592,50,282}$=0.456
		p=0.513	p=0.462	p=0.748
		$n_p{}^2$=0.031	$n_p{}^2$=0.061	$n_p{}^2$=0.032
Standard deviation	AP	$F_{1,14}$**=16.012**	$F_{5,70}$=1.431	$F_{5,70}$=1.429
		p=0.001	p=0.224	p=0.225
		$n_p{}^2$**=0.534**	$n_p{}^2$=0.093	$n_p{}^2$=0.093
	ML	$F_{1,14}$=3.748	$F_{5,70}$=1.078	$F_{5,70}$=1.853
		p=0.073	p=0.380	p=0.114
		$n_p{}^2$=0.211	$n_p{}^2$=0.072	$n_p{}^2$=0.117
Variance	AP	$F_{1,14}$**=14.310**	$F_{5,70}$=1.287	$F_{5,70}$=1.301
		p=0.002	p=0.279	p=0.274
		$n_p{}^2$**=0.505**	$n_p{}^2$=0.084	$n_p{}^2$=0.085
	ML	$F_{1,14}$=1.474	$F_{5,70}$=0.722	$F_{5,70}$=1.821
		p=0.245	p=0.609	p=0.120
		$n_p{}^2$=0.095	$n_p{}^2$=0.049	$n_p{}^2$=0.115
Root mean square	AP	$F_{1,14}$=4.047	$F_{5,70}$=0.365	$F_{5,70}$=0.331
		p=0.064	p=0.871	p=0.893
		$n_p{}^2$=0.224	$n_p{}^2$=0.025	$n_p{}^2$=0.023
	ML	$F_{1,14}$**=16.506**	$F_{5,70}$=1.828	$F_{5,70}$=1.676
		p=0.010	p=0.119	p=0.152
		$n_p{}^2$**=0.388**	$n_p{}^2$=0.115	$n_p{}^2$=0.107
Interquartile range	AP	$F_{1,14}$**=9.262**	$F_{5,70}$=1.676	$F_{5,70}$=0.959
		p=0.009	p=0.152	p=0.449
		$n_p{}^2$**=0.398**	$n_p{}^2$=0.107	$n_p{}^2$=0.064
	ML	$F_{1,14}$=4.049	$F_{5,70}$=0.868	$F_{5,70}$=1.788
		p=0.064	p=0.507	p=0.127
		$n_p{}^2$=0.224	$n_p{}^2$=0.058	$n_p{}^2$=0.113
Signal distance	AP	$F_{1,14}$=3.300	$F_{2.023,28.323}$**=8.586**	$F_{2.023,28.323}$=0.700
		p=0.091	**p=0.001**	p=0.507
		$n_p{}^2$=0.191	$n_p{}^2$**=0.380**	$n_p{}^2$=0.048
	ML	$F_{1,14}$=3.228	$F_{2.011,28.156}$**=8.708**	$F_{2.011,28.156}$=0.631
		p=0.094	**p=0.001**	p=0.540
		$n_p{}^2$=0.187	$n_p{}^2$**=0.383**	$n_p{}^2$=0.043

In bold are identified the statistically different results.

Table B.3: Results from Two-way repeated-measures ANOVA for linear measures with no statistical significance.

Metrics		**Group**	**Week**	**Week x Group**
Sway range		$F_{1,14}$=1.788	$F_{5,70}$=0.786	$F_{5,70}$=0.202
		p=0.203	p=0.563	p=0.961
		$n_p{}^2$=0.113	$n_p{}^2$=0.053	$n_p{}^2$=0.014
	AP	$F_{1,14}$=1.070	$F_{5,70}$=0.720	$F_{5,70}$=0.294
		p=0.318	p=0.611	p=0.915
		$n_p{}^2$=0.071	$n_p{}^2$=0.049	$n_p{}^2$=0.021
	ML	$F_{1,14}$=1.790	$F_{5,70}$=0.839	$F_{5,70}$=0.121
		p=0.202	p=0.527	p=0.987
		$n_p{}^2$=0.113	$n_p{}^2$=0.057	$n_p{}^2$=0.009
Sway area		$F_{1,14}$=0.277	$F_{5,70}$=1.100	$F_{5,70}$=0.369
		p=0.607	p=0.368	p=0.868
		$n_p{}^2$=0.019	$n_p{}^2$=0.073	$n_p{}^2$=0.026
Sway path		$F_{1,14}$=0.548	$F_{5,70}$=0.979	$F_{5,70}$=0.441
		p=0.471	p=0.437	p=0.819
		$n_p{}^2$=0.038	$n_p{}^2$=0.065	$n_p{}^2$=0.031
Sway velocity		$F_{1,14}$=0.546	$F_{5,70}$=0.613	$F_{5,70}$=0.341
		p=0.472	p=0.690	p=0.886
		$n_p{}^2$=0.038	$n_p{}^2$=0.042	$n_p{}^2$=0.024
Sway distance		$F_{1,14}$=0.412	$F_{5,70}$=0.370	$F_{5,70}$=0.444
		p=0.531	p=0.868	p=0.816
		$n_p{}^2$=0.029	$n_p{}^2$=0.026	$n_p{}^2$=0.031
Mean	AP	$F_{1,14}$=0.533	$F_{5,70}$=1.461	$F_{5,70}$=0.466
		p=0.477	p=0.214	p=0.800
		$n_p{}^2$=0.037	$n_p{}^2$=0.094	$n_p{}^2$=0.032
	ML	$F_{1,14}$=0.638	$F_{5,70}$=1.713	$F_{5,70}$=1.061
		p=0.438	p=0.143	p=0.389
		$n_p{}^2$=0.044	$n_p{}^2$=0.109	$n_p{}^2$=0.70
Autocorrelation	AP	$F_{1,14}$=1.550	$F_{5,70}$=0.462	$F_{5,70}$=0.741
		p=0.234	p=0.803	p=0.595
		$n_p{}^2$=0.100	$n_p{}^2$=0.032	$n_p{}^2$=0.050
	ML	$F_{1,14}$=2.614	$F_{5,70}$=1.695	$F_{5,70}$=1.020
		p=0.128	p=0.147	p=0.413
		$n_p{}^2$=0.157	$n_p{}^2$=0.108	$n_p{}^2$=0.068
Median	AP	$F_{1,14}$=0.601	$F_{5,70}$=1.294	$F_{5,70}$=0.567
		p=0.451	p=0.277	p=0.725
		$n_p{}^2$=0.041	$n_p{}^2$=0.085	$n_p{}^2$=0.039
	ML	$F_{1,14}$=0.417	$F_{5,70}$=1.605	$F_{5,70}$=1.229
		p=0.529	p=0.170	p=0.305
		$n_p{}^2$=0.029	$n_p{}^2$=0.103	$n_p{}^2$=0.081

Appendix C

Nonlinear results

In the next pages are presented:

1. Figures C.1 and C.2: Additional results graphs of the nonlinear metrics without statistically significant differences;
2. Table C.1: Results table for each calculated metric, with the Mean±SD values, and the p-values for the two-way repeated-measures ANOVA between and whiting groups;
3. Tables C.2 and C.3: Results from the two-way repeated-measures ANOVA, all the metrics calculated, presented first the ones with statistically significant differences.

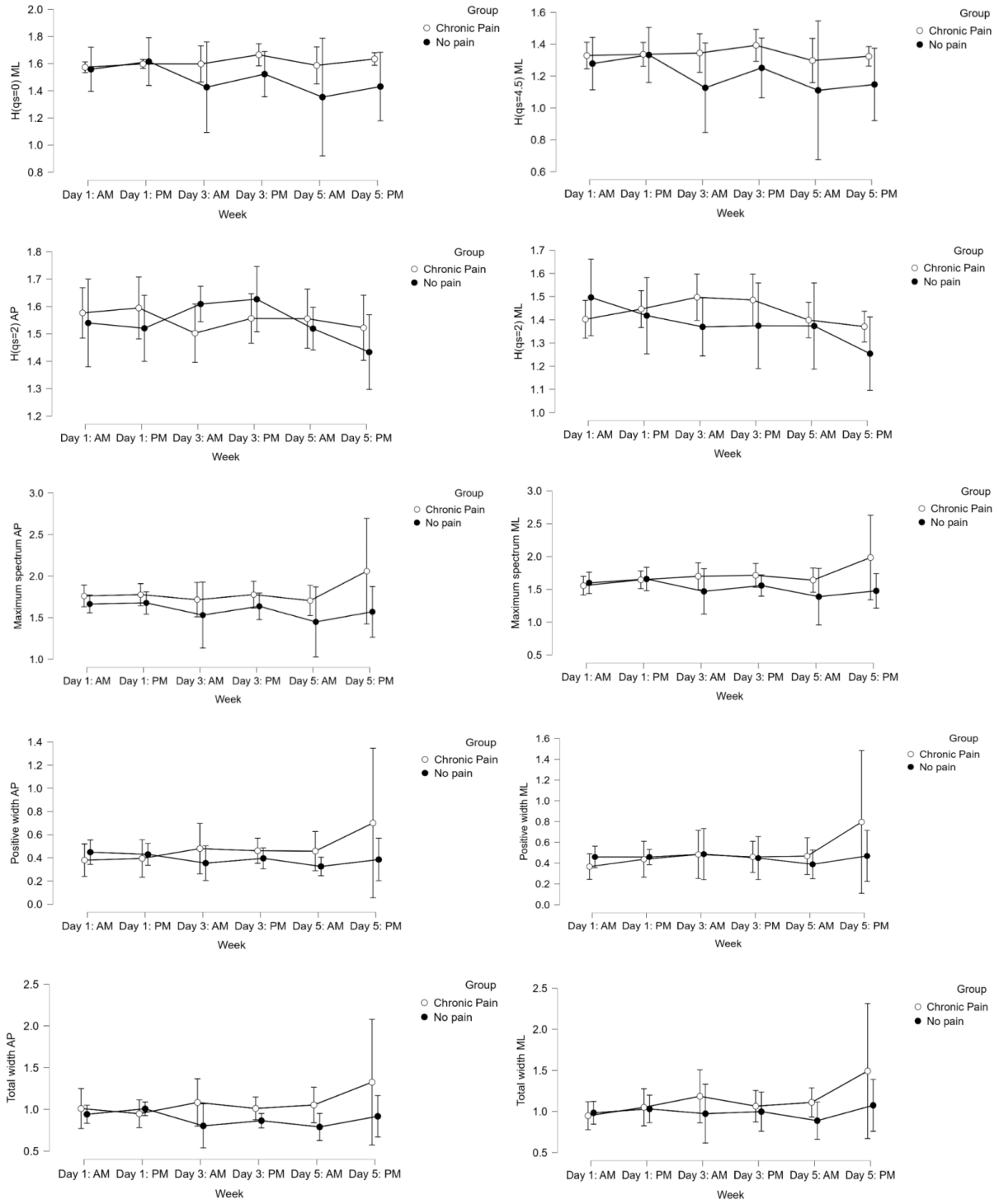

Figure C.1: Nonlinear metrics evolution over the day and week for the ones without statistical significance.

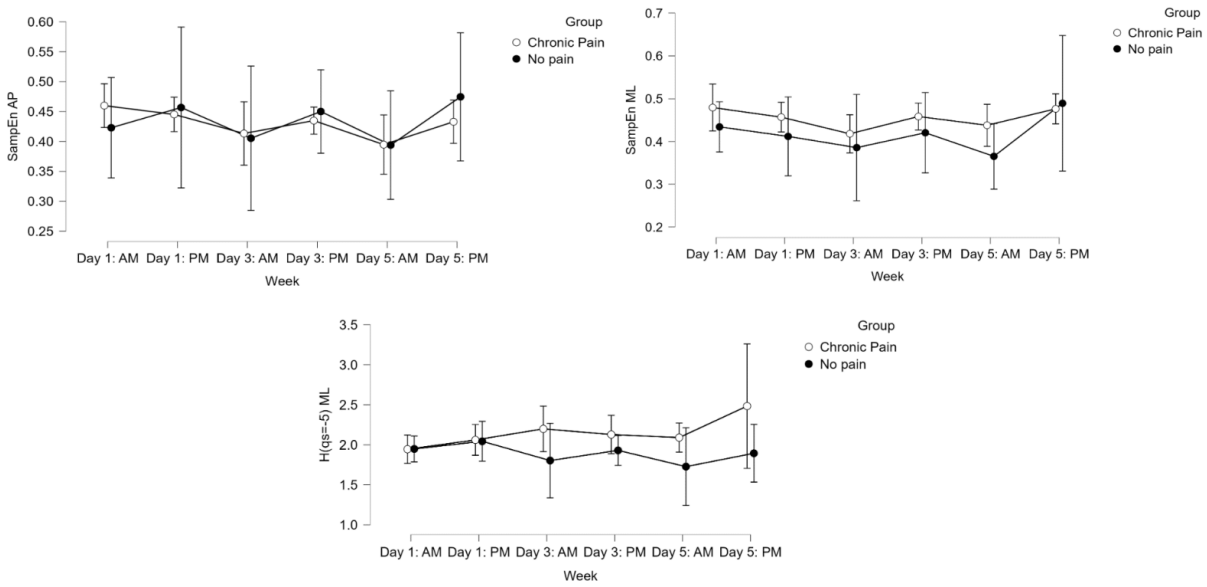

Figure C.2: Nonlinear metrics evolution over the day and week for the ones without statistical significance. (cont.)

Table C.1: Results [Mean±SD] for calculated Nonlinear measures with p-values for within and between subjects comparison.

Metric	**Day/Time**												**WG**	**BG**
	CG						**EG**						**p**	**p**
	Day 1		**Day 3**		**Day 5**		**Day 1**		**Day 3**		**Day 5**			
	AM	**PM**	**AM**	**PM**	**AM**	**PM**	**AM**	**PM**	**AM**	**PM**	**AM**	**PM**		
$H_{qs=2}$ (AP)	1.54±0.18	1.52±0.11	1.61±0.15	1.63±0.16	1.52±0.10	1.43±0.15	1.58±0.15	1.60±0.11	1.50±0.18	1.56±0.12	1.56±0.18	1.52±0.17	0.34	0.82
$H_{qs=2}$ (ML)	1.50±0.19	1.42±0.16	1.37±0.18	1.37±0.15	1.37±0.11	1.25±0.18	1.40±0.12	1.45±0.11	1.50±0.16	1.49±0.16	1.40±0.09	1.37±0.12	0.07	0.16
$H_{qs=-5}$ (AP)	1.98±0.26	2.06±0.13	1.83±0.54	1.95±0.22	1.76±0.58	1.92±0.25	2.19±0.13	2.15±0.13	2.13±0.35	2.15±0.14	2.11±0.31	2.49±1.16	0.48	**0.04***
$H_{qs=-5}$ (ML)	1.95±0.27	2.04±0.08	1.80±0.58	1.93±0.30	1.73±0.57	1.89±0.23	1.94±0.23	2.06±0.13	2.20±0.35	2.13±0.18	2.09±0.23	2.48±1.2	0.50	0.05
$H_{qs=0}$ (AP)	1.63±0.20	1.64±0.08	1.50±0.46	1.60±0.21	1.41±0.45	1.53±0.19	1.71±0.12	1.74±0.08	1.63±0.23	1.73±0.09	1.66±0.21	1.73±1.00	0.21	**0.04***
$H_{qs=0}$ (ML)	1.56±0.22	1.62±0.07	1.43±0.45	1.52±0.27	1.35±0.47	1.43±0.15	1.57±0.07	1.60±0.08	1.60±0.19	1.67±0.11	1.59±0.18	1.64±0.07	0.33	0.07
$H_{qs=4.5}$ (AP)	1.36±0.22	1.40±0.06	1.29±0.38	1.36±0.19	1.21±0.38	1.30±0.13	1.50±0.12	1.50±0.08	1.37±0.20	1.45±0.07	1.38±0.21	1.48±0.08	0.20	**0.02***
$H_{qs=4.5}$ (ML)	1.28±0.23	1.33±0.07	1.13±0.40	1.25±0.27	1.11±0.45	1.15±0.11	1.33±0.14	1.34±0.10	1.35±0.18	1.39±0.10	1.30±0.21	1.32±0.08	0.30	0.05
Total width (AP)	0.94±0.22	1.01±0.21	0.80±0.30	0.87±0.19	0.79±0.31	0.92±0.20	1.01±0.19	0.95±0.18	1.08±0.30	1.01±0.16	1.05±0.27	1.33±1.15	0.57	0.10
Total width (ML)	0.98±0.17	1.03±0.08	0.97±0.31	1.00±0.26	0.89±0.30	1.08±0.34	0.95±0.22	1.05±0.12	1.19±0.34	1.06±0.13	1.11±0.23	1.49±1.26	0.39	0.17
Positive width (AP)	0.45±0.11	0.43±0.16	0.36±0.17	0.40±0.14	0.33±0.16	0.39±0.16	0.38±0.12	0.40±0.15	0.48±0.19	0.46±0.11	0.46±0.17	0.70±0.98	0.59	0.27
Positive width (ML)	0.46±0.10	0.46±0.05	0.49±0.16	0.45±0.23	0.39±0.19	0.47±0.25	0.37±0.18	0.44±0.11	0.48±0.21	0.46±0.08	0.47±0.14	0.80±1.04	0.46	0.52
Negative width (AP)	0.49±0.13	0.58±0.09	0.45±0.13	0.47±0.07	0.46±0.17	0.53±0.12	0.63±0.12	0.55±0.10	0.60±0.15	0.55±0.10	0.60±0.13	0.63±0.18	0.50	**0.02***
Negative width (ML)	0.52±0.15	0.57±0.08	0.49±0.20	0.55±0.09	0.50±0.15	0.61±0.11	0.58±0.10	0.61±0.13	0.70±0.16	0.60±0.10	0.64±0.14	0.70±0.23	0.43	**0.02***
Maximum spectrum (AP)	1.66±0.20	1.68±0.09	1.53±0.47	1.64±0.21	1.45±0.46	1.57±0.20	1.76±0.12	1.78±0.08	1.72±0.27	1.78±0.09	1.71±0.22	2.06±0.98	0.46	0.06
Maximum spectrum (ML)	1.60±0.22	1.66±0.07	1.47±0.46	1.56±0.27	1.39±0.47	1.48±0.16	1.56±0.20	1.65±0.09	1.70±0.24	1.71±0.12	1.64±0.18	1.98±0.99	0.53	0.09
Sample Entropy (AP)	0.42±0.07	0.46±0.10	0.41±0.13	0.45±0.07	0.39±0.14	0.48±0.13	0.46±0.06	0.45±0.05	0.41±0.06	0.44±0.03	0.40±0.08	0.43±0.06	0.19	0.87
Sample Entropy (ML)	0.43±0.07	0.41±0.06	0.39±0.11	0.42±0.05	0.37±0.11	0.49±0.18	0.48±0.08	0.46±0.05	0.42±0.06	0.46±0.04	0.44±0.08	0.48±0.04	0.08	0.09

Abbreviations WG: Within Group; BG: Between Group; *: indicates p<0.05

Table C.2: Results from Two-way repeated-measures ANOVA for statistically significant nonlinear measures.

Metrics		**Group**	**Week**	**Week x Group**
$H_{qs=-5}$	AP	$F_{1,14}$**=5.478**	$F_{1.668,23.359}$=0.707	$F_{1.668,23.359}$=0.521
		p=0.035	p=0.479	p=0.569
		$n_p{}^2$**=0.281**	$n_p{}^2$=0.048	$n_p{}^2$=0.036
	ML	$F_{1,14}$=4.495	$F_{1.648,23.067}$=0.667	$F_{1.648,23.067}$=0.946
		p=0.052	p=0.495	p=0.387
		$n_p{}^2$=0.243	$n_p{}^2$=0.045	$n_p{}^2$=0.063
$H_{qs=0}$	AP	$F_{1,14}$**=4.837**	$F_{2.167,30.344}$=1.651	$F_{2.167,30.344}$=0.375
		p=0.045	p=0.207	p=0.707
		$n_p{}^2$**=0.257**	$n_p{}^2$=0.105	$n_p{}^2$=0.026
	ML	$F_{1,14}$=3.736	$F_{2.196,30.741}$=1.179	$F_{2.196,30.741}$=1.152
		p=0.074	p=0.325	p=0.333
		$n_p{}^2$=0.211	$n_p{}^2$=0.078	$n_p{}^2$=0.076
$H_{qs=4.5}$	AP	$F_{1,14}$**=6.548**	$F_{2.340,32.762}$=1.651	$F_{2.340,32.762}$=0.218
		p=0.023	p=0.204	p=0.838
		$n_p{}^2$**=0.319**	$n_p{}^2$=0.105	$n_p{}^2$=0.015
	ML	$F_{1,14}$=4.478	$F_{2.842,39.794}$=1.262	$F_{2.842,39.794}$=0.764
		p=0.053	p=0.300	p=0.514
		$n_p{}^2$=0.242	$n_p{}^2$=0.083	$n_p{}^2$=0.052
Negative width	AP	$F_{1,14}$**=6.428**	$F_{3.447,48.257}$=0.826	$F_{3.447,48.257}$=1.174
		p=0.024	p=0.500	p=0.332
		$n_p{}^2$**=0.315**	$n_p{}^2$=0.056	$n_p{}^2$=0.077
	ML	$F_{1,14}$**=6.716**	$F_{3.023,42.325}$=0.937	$F_{3.023,42.325}$=0.937
		p=0.021	p=0.432	p=0.432
		$n_p{}^2$**=0.324**	$n_p{}^2$=0.063	$n_p{}^2$=0.063

In bold are identified the statistically different results.

Table C.3: Results from Two-way repeated-measures ANOVA for nonlinear measures with no statistical significance.

Metrics		**Group**	**Week**	**Week x Group**
$H_{qs=2}$	AP	$F_{1,14}$=0.053	$F_{5,70}$=1.163	$F_{5,70}$=1.291
		p=0.821	p=0.336	p=0.278
		$n_p{}^2$=0.004	$n_p{}^2$=0.077	$n_p{}^2$=0.084
	ML	$F_{1,14}$=2.217	$F_{5,70}$=2.125	$F_{5,70}$=1.468
		p=0.159	p=0.072	p=0.211
		$n_p{}^2$=0.137	$n_p{}^2$=0.132	$n_p{}^2$=0.095
Total width	AP	$F_{1,14}$=3.062	$F_{1.401,19.611}$=0.452	$F_{1.401,19.611}$=0.592
		p=0.102	p=0.574	p=0.505
		$n_p{}^2$=0.179	$n_p{}^2$=0.031	$n_p{}^2$=0.041
	ML	$F_{1,14}$=2.085	$F_{1.393,19.499}$=0.890	$F_{1.393,19.499}$=0.485
		p=0.171	p=0.391	p=0.556
		$n_p{}^2$=0.130	$n_p{}^2$=0.060	$n_p{}^2$=0.034
Positive width	AP	$F_{1,14}$=1.328	$F_{1.233,17.259}$=0.371	$F_{1.233,17.259}$=0.597
		p=0.268	p=0.594	p=0.484
		$n_p{}^2$=0.087	$n_p{}^2$=0.026	$n_p{}^2$=0.041
	ML	$F_{1,14}$=0.431	$F_{1.285,17.984}$=0.682	$F_{1.285,17.984}$=0.571
		p=0.522	p=0.456	p=0.501
		$n_p{}^2$=0.030	$n_p{}^2$=0.046	$n_p{}^2$=0.039
Maximum spectrum	AP	$F_{1,14}$=4.390	$F_{1.585,22.195}$=0.749	$F_{1.585,22.195}$=0.595
		p=0.055	p=0.455	p=0.523
		$n_p{}^2$=0.239	$n_p{}^2$=0.051	$n_p{}^2$=0.041
	ML	$F_{1,14}$=3.400	$F_{1.617,22.631}$=0.580	$F_{1.617,22.631}$=1.058
		p=0.086	p=0.533	p=0.350
		$n_p{}^2$=0.195	$n_p{}^2$=0.040	$n_p{}^2$=0.070
Sample Entropy	AP	$F_{1,14}$=0.028	$F_{3.387,47.424}$=1.644	$F_{3.387,47.424}$=0.479
		p=0.869	p=0.187	p=0.721
		$n_p{}^2$=0.002	$n_p{}^2$=0.105	$n_p{}^2$=0.033
	ML	$F_{1,14}$=3.361	$F_{2.643,37.004}$=2.534	$F_{2.643,37.004}$=0.497
		p=0.088	p=0.079	p=0.663
		$n_p{}^2$=0.194	$n_p{}^2$=0.153	$n_p{}^2$=0.034